

Review

Chemistry of coordination space of porous coordination polymers

Susumu Kitagawa^{a,*}, Ryotaro Matsuda^b^a Department of Synthetic Chemistry and Biological Chemistry, Kyoto University, Katsura, Nishikyo-ku, Kyoto 615-8510, Japan^b Institute for Materials Chemistry and Engineering, Kyushu University, 6-1 Kasuga-koen, Kasuga, Fukuoka 816-8580, Japan

Received 8 February 2007; accepted 21 July 2007

Available online 1 August 2007

Contents

1. Introduction	2491
1.1. What is coordination space?	2491
1.2. Designability, regularity and flexibility of porous coordination polymers	2491
2. Closed space of coordination pillared layer (CPL) structures	2493
2.1. Structure of CPL type porous coordination polymers	2493
2.2. Adsorption in periodic regular one-dimensional channels of CPL-1	2495
2.3. Formation of molecular arrays in CPL-1	2496
2.4. Molecular arrays of different shaped guest molecules in CPL-1	2497
2.5. Effect of periodic electric field of the pore	2497
2.6. Strong confinement effect enhanced by regularly aligned functional groups in nanochannel	2498
3. Flexible nature of coordination polymers	2500
3.1. The guideline for flexible network	2500
3.2. Bond elongation and shortening or cleavage and reformation	2500
3.3. Sponge-like structural transformation	2502
3.4. Rotational motion of aromatic rings	2504
4. Perspectives	2506
4.1. Cooperative properties with functional framework and guest molecules	2507
4.2. Low-dimensional form—thin layer compounds	2507
4.3. Mesoscale compounds	2507
4.4. Introduction of anisotropy	2507
4.5. Redox frameworks	2507
Acknowledgements	2507
References	2507

Abstract

Recently, syntheses of epoch-making space materials using coordination compounds are underway by various groups. The rational synthetic strategy of the space of coordination compounds provides unique structures and functions, which have not been found in traditional materials. Now, we intend to focus on this scientific field from a new viewpoint. We define *coordination space* as the space where the coordination bond plays an important role in the formation of the spatial structures and where various physical properties are exhibited. In this article, we focus on the *coordination spaces* provided by porous coordination polymers, and their uniqueness is illustrated with current representative results.

© 2007 Elsevier B.V. All rights reserved.

Keywords: Coordination space; Porous coordination polymer; Adsorption; Uniform channel structure; Flexible framework; Direct observation of confined guest molecules

* Corresponding author. Tel.: +81 75 383 2733; fax: +81 75 383 2732.

E-mail address: kitagawa@sbchem.kyoto-u.ac.jp (S. Kitagawa).

1. Introduction

1.1. What is coordination space?

Material and life sciences have contributed to human well-being and prosperity, and atoms and molecules play a central role in this respect. The syntheses of molecules have been a major theme in the previous century. Molecules are architectures composed of atoms, while the supramolecular chemistry developed in the last century deals with architectures built from molecules, paving the way for nanoscience [1]. In addition to the framework entity, space surrounded and partitioned by atoms and molecules could be another world of science. If we build nanosized spaces *ad arbitrium*, what kind of materials can be created and what discoveries for molecules in the space can be made? In a nanosized world, walls, which are composed of atoms and molecules and apportioned space, have a considerable effect on orientation, correlation, and assembled structure of guest molecules. We can, therefore, control such states of the guest molecules by changing the shapes and materials of walls. When molecules are confined in a space and undergo stress caused by a deviation from thermodynamically and kinetically stable structures of the ambient surroundings, such stress brings about effective energy conversion and new chemical reactions. Space apportioned by atoms and molecules creates new functions based on its shape and dynamics characteristic of the nanoworld. At the end of the last century, we chemists focused on supramolecular frameworks composed of molecules, while in the 21st century we are opening up a new era of nanospace chemistry by creating various types of spaces (Fig. 1). We have to develop new synthetic routes to build the desired nanosized space effectively and on a large scale, and this is a basic methodology required for nanotechnologies. The most practical methods to build nanosized space are chemical self-assembly and self-organization, and coordination bonds are the key to the development of the required new synthetic technologies. Coordination bonds are not as strong as covalent bonds and not as weak as hydrogen bonds. Constituent organic molecules and metal ions are assembled into a variety of spatial structures under mild conditions. In this area we minutely design molecules to build space that gives an opportunity to find new phenomena based on molecular coagulation, molecular stress, and activation of molecules (Fig. 2). For this purpose, we need to develop a new chemistry that allows us to control structures and functionality of spaces. Space motifs built by molecular blocks are: (1) reactions of metal ions (connector) with organic ligands (linker) to give coordination crystals with infinite structures. We can build spaces with different sizes composed of several or tens of molecules. (2) Surfaces of bulk material and nanoparticles can be recognized as coordination space. (3) The coordination space of metal complexes embedded in a protein has the hidden possibility of a new functionalized space.

Currently, the syntheses of epoch-making space materials are underway by various groups. Collaborations by these researchers have led to the establishment of rational synthetic strategies of coordination space, which have a variety of functions. In nanospace built for energy storage and transfer, we

can control and create chemical and physical functions such as charge separations and proton transfers. Molecules and aggregates trapped in nanospace may have the potential to show physical properties based on quantum effects. This area is intended to focus on the scientific field from the new viewpoint (coordination space), which has not been seen in traditional chemistry and physics, by organizing the research groups from coordination chemistry, bioinorganic chemistry, catalytic chemistry, electrochemistry, and solid-state physics. We could define *coordination space* as those spaces where the coordination bond plays an important role in the formation of the spatial structures and where various physical properties are exhibited. The mission in this field is to explore (1) a new synthetic method to control nanosize space (nanospace) precisely, (2) various novel *Nanospace Materials*, and (3) magnetic, dielectric and optical properties, reactivity, and catalytic functionality, which are characteristic of the molecular systems in nanospace. In particular, we focus on previously unknown phenomena such as condensation of molecules, molecular stresses, and activation of molecules that may occur in these spaces. This article focuses on porous coordination polymers, whose cavities are readily functionalized by molecular building blocks and coordination bonds as a linking force. Their uniqueness is illustrated with current representative results.

1.2. Designability, regularity and flexibility of porous coordination polymers

Porous compounds have attracted the attention of chemists, physicists and materials scientists due to scientific interest in the creation of nanometer-sized spaces and the observation of novel phenomena therein. Commercial interest includes their application in separation, storage, and heterogeneous catalysis. Until the mid-1990s, there were basically two types of porous materials, namely, inorganic and carbon-based materials. In the case of microporous inorganic solids, the largest two subclasses are the aluminosilicates and aluminophosphates. Zeolites are 3D crystalline, hydrated alkaline or alkaline earth aluminosilicates with the general formula $M_{x/n}^{n+}[(AlO_2)_x(SiO_2)_y]^{x-} \cdot wH_2O$ [2,3]. The activated carbons have a high open porosity and high specific surface area, but have a disordered structure, the essential feature of which is a twisted network of defective hexagonal carbon layers, cross-linked by aliphatic bridging groups.

On the other hand, porous coordination polymers (PCPs), beyond the scope of the former two porous materials have recently appeared. These porous coordination polymers have an infinite network with backbones constructed by metal ions as connectors and ligands as linkers, and form a family of “inorganic and organic hybrid polymers” [4–31], which are also called porous metal-organic frameworks (MOFs). The structural integrity of the building units, which can be maintained throughout the reactions, allows for their use as modules in the assembly of extended structures. Werner complexes, β -M(4-methylpyridyl)₄(NCS)₂ (M = Ni(II) or Co(II)) [32], Prussian blue compounds [33–35], and Hofmann clathrates and their derivatives have frameworks that are built of CN-linkages between square-planar or tetrahedral tetracyanometallate(II)

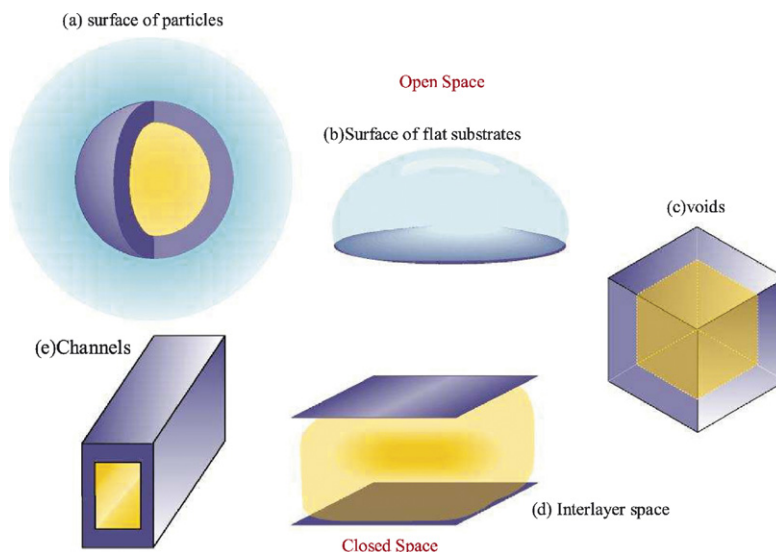


Fig. 1. Variety of spaces. Open space (a and b) and closed space (c–e).

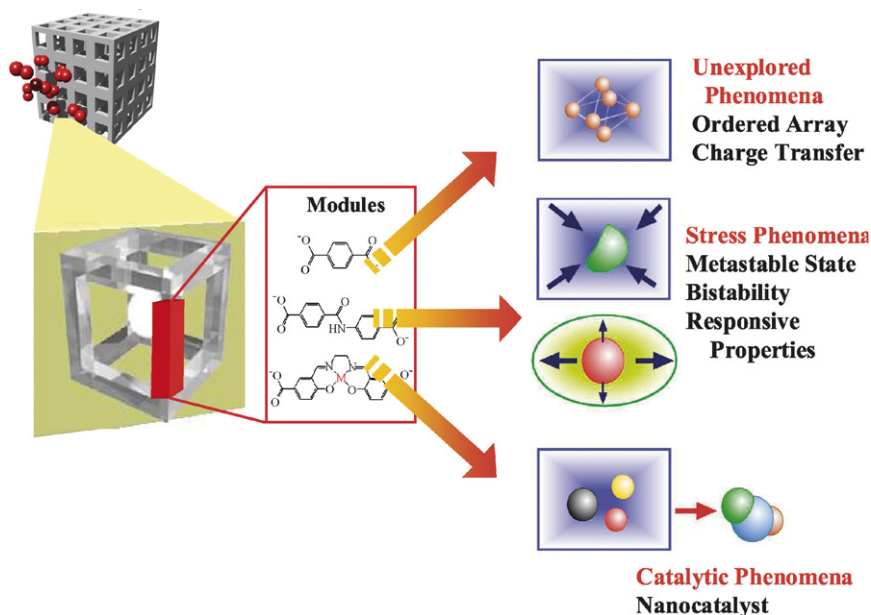


Fig. 2. Various functions of closed space.

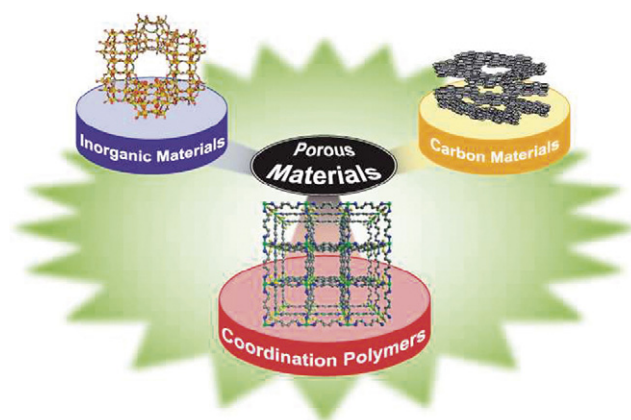


Fig. 3. Classes of porous materials (figure was reproduced from Ref. [10], with permission of the copyright holders).

units and octahedral metal(II) units coordinated by complementary ligands [35–37], which are known to be materials that can reversibly absorb small molecules. An early study reports the use of an organic bridging ligand to form the porous coordination polymer $[\text{Cu}(\text{NO}_3)(\text{adiponitrile})_2]_n$ with a diamond net, however, the adsorption behavior was not reported [38]. Since the early 1990s, research on the structures of porous coordination polymers has increased greatly, and some examples with functional micropores have started to appear. The structural entity of the cavity could be related to a porous property. In 1990, Robson et al. reported a porous coordination polymer capable of anion-exchange [39]. Subsequently, the catalytic properties of a 2D $\text{Cd}(\text{II})$ -4,4'-bpy (bpy = bipyridine) coordination polymer were studied by Fujita et al. in 1994 [40]. In 1995, a guest adsorption was studied by Yaghi's [41] and Moore's groups [42]. The

robustness of the structure after removal of guest molecules was remarkable because recrystallization is the preferable way for exchange/removal–inclusion of guest molecules or ions. Ultimately, gas adsorption at ambient temperature was carried out in 1997 by Kitagawa's group [43]. Thus recrystallization is not the necessary procedure for PCPs. Since then, the robustness of PCPs has been accepted and PCPs were recognized as porous compounds. In a surprisingly short period, their structural chemistry have matured dramatically. A survey of the research published in recent years shows an extraordinary increase in the number of articles. Now, they are gaining an important position in the field of porous materials and add a new category to the conventional classification (Fig. 3). The following three features would be most pivotal advantages, namely (1) designability, (2) regularity and (3) flexibility.

- (1) High designability: the key to success to obtain highly functional materials is design of the desired architectural, chemical, and physical properties of the resulting solid-state compounds. One can take advantages in the design of PCPs because the reactions of the PCPs mostly occur at mild conditions and choice of a certain combination of discrete building units leads with a high probability to a desired extended network.
- (2) Regularity: regular pore distribution in a microporous solid is important for adsorption phenomena because when the size of the micropore is comparable to that of a guest molecule, the periodic potential from the pore wall could influence the form and orientation of the adsorbed guest molecules. Regular pore distribution can be readily realized for coordination polymers as well as inorganic porous materials. The micropores of coordination polymers have a regular periodical structure due to their crystalline form, which affords a periodic potential on their channel surface. The structural relationships between adsorbed guest molecules and host frameworks (e.g. (1) position of guest molecules in the channel, (2) the assembled structure of guest molecules in the channel, (3) the influence of guest molecules on the channel structure are key subjects for understanding the adsorption behavior and the physical or chemical properties of adsorbed guest molecules in nanochannels. In addition, molecules confined in a *uniform* restricted nanospace form molecular assemblies and afford unique group properties that are not realized in the bulk state.
- (3) Flexibility: many recent reports on the dynamic properties on porous coordination polymers, reveal that they are much more flexible than generally believed. Dynamic pores could come from a sort of “soft” framework with bistability, whose two states go back and forth to one of two counterparts; a system could exist in one or two states for the same external field parameter values. The structural rearrangement of molecules proceeds from the “closed” phase to the “open” phase responding to the guest molecules. Some porous coordination polymers have such flexibility, and they can be developed as a unique class of materials such as highly selective gas sensors or gas separation compounds,

which could not be obtained in a rigid porous material. Dynamic structural transformations based on these flexible frameworks are one of the most interesting phenomena, presumably characteristic of coordination polymers, so-called “3rd generation” porous coordination polymers [20]. Based on a number of flexible porous coordination polymers and their dynamic properties, we proposed a synthetic guideline for them, which will be presented in Section 3.

2. Closed space of coordination pillared layer (CPL) structures

2.1. Structure of CPL type porous coordination polymers

In this section, we focus on a series of compounds as porous coordination pillared layer structures (CPLs), $[\text{Cu}_2(\text{pzdc})_2(\text{P})]_n$ (pzdc = pyrazine-2,3-dicarboxylate, P = pillar ligands) [44–54]. The CPL series is one representative example of porous coordination polymers with high designability. The channel dimensions (size and shape) and surface functionality of the CPLs can be controlled systematically by modification of pillar ligands (P) (Fig. 4). In addition, CPLs are also one of the best candidates to realize low-dimensional assemblies of the guest molecules; because (1) the one-dimensional channels in CPLs have a precise potential periodicity due to their crystal form, and this provides well-regulated and well-organized molecular assemblies, and (2) the pore dimension and surface functionalities can be controlled simply by changing the pillar ligands (P); thus, we can control size and form of guest molecular assemblies.

The CPL compounds are synthesized by a simple procedure; a mixture of ethanol and water solutions of Na_2pzdc and the pillar ligand (P) is slowly added to the H_2O solu-

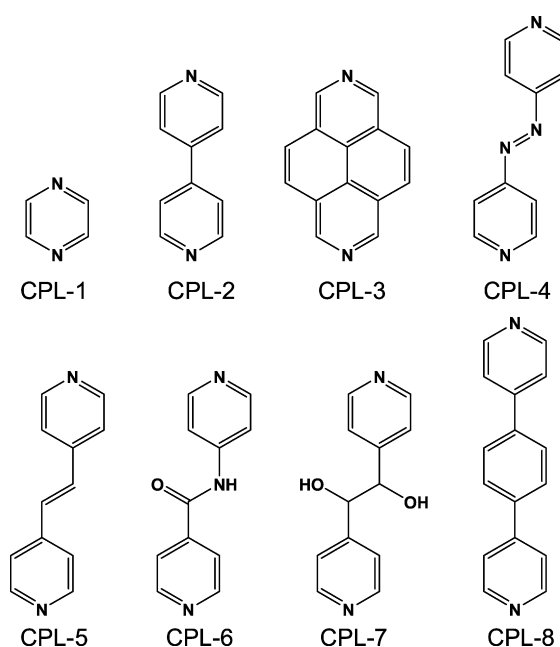


Fig. 4. Pillar ligands.

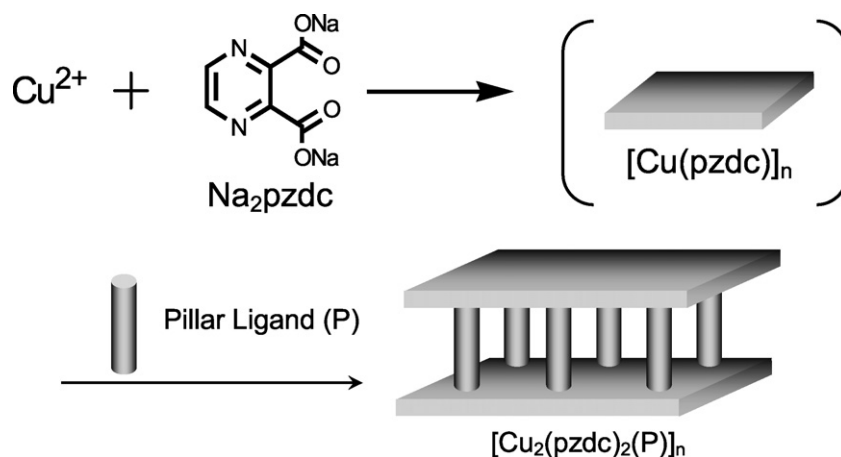


Fig. 5. Synthetic scheme of CPL.

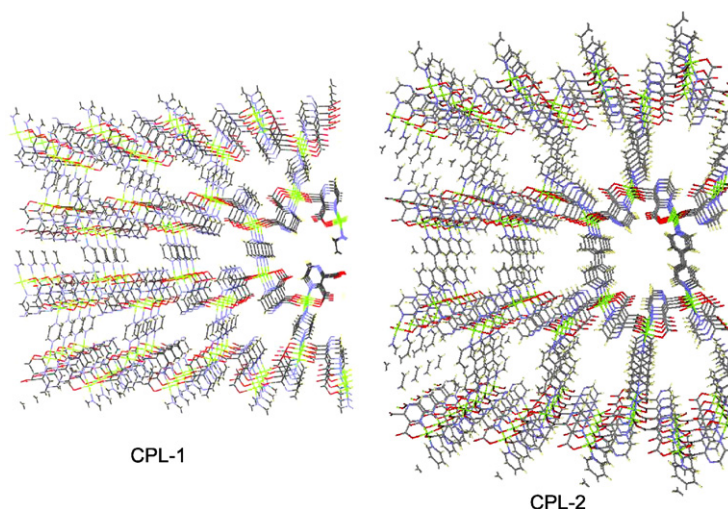


Fig. 6. Perspective views of crystal structures of CPL-1 and CPL-2 along the channel direction.

tion containing Cu(II) ion at room temperature in air. Stirring for 1-day provides the desired compounds in good yield (Fig. 5).

In the CPL structure (Fig. 6) the pzdc units link the three crystallographically equivalent copper atoms (Cu(1), Cu(2), and Cu(3)), as shown in Fig. 7. The N(1), and O(1) atoms of carboxyl group(1) chelates the Cu(1) atom. The carboxyl group(2) bridges Cu(2) and Cu(3) atoms in such a fashion that the O(3) and O(4) atoms sit at the apical and equatorial positions, respectively. The remaining N(2) and O(2) atoms have no interaction with any other atoms. As a result, a neutral two-dimensional layer of $[\text{Cu}(\text{pzdc})]_n$ forms in the *ac* plane, as shown in Fig. 8. These layers are connected by pillar ligands, resulting in a 3D pillared layer structure. Many atoms exist densely in the two-dimensional layer spread out in the *ac* plane. Guest molecules cannot pass through this plane thus the translational motion of guest molecules along the *b*-axis is forbidden. The pillar ligands are aligned closely along the *a*-axis. The space between the nearest pillar ligands is less than 0.5 Å assuming van der Waals radii, and therefore, the translational motion of guest molecules along the *c*-axis is also forbidden. On the other hand, there is large

enough space for molecules passing along the *a*-axis. As a result, these CPL series are regarded as one-dimensional channel materials, which are suitable for the formation of low-dimensional assemblies of small guest molecules.

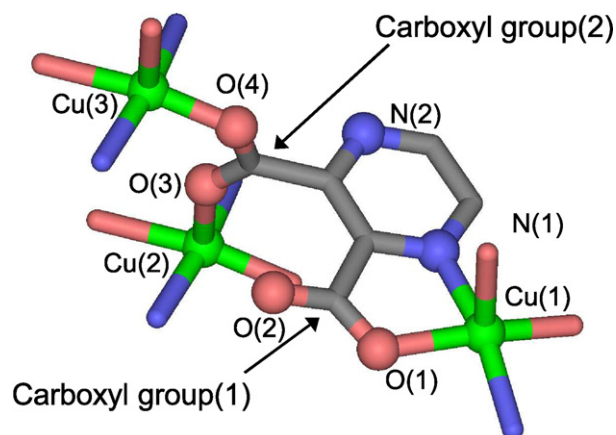


Fig. 7. View of the coordination geometry around copper ions of CPL-1.

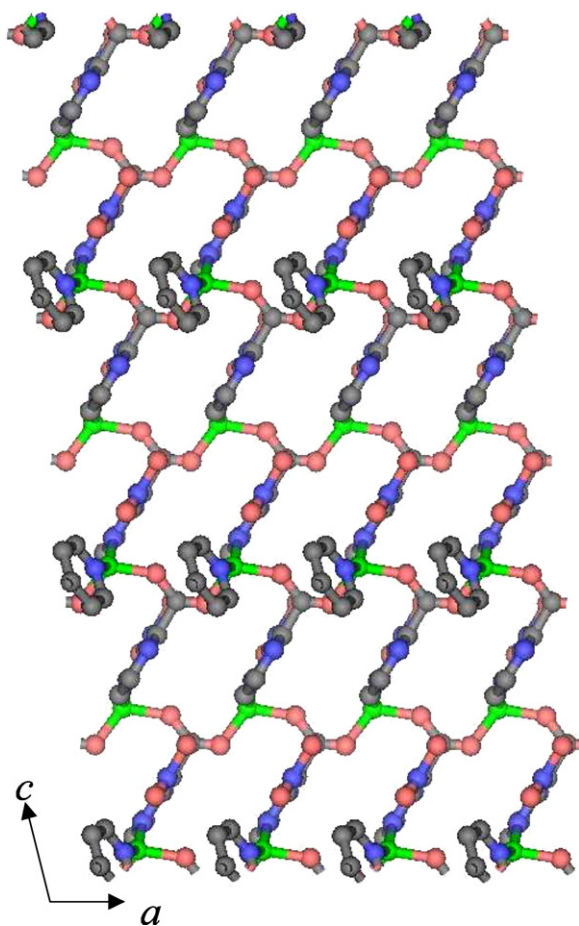


Fig. 8. View of the two-dimensional layers of CPL-1 (figure was reproduced from Ref. [48], with permission of the copyright holders).

2.2. Adsorption in periodic regular one-dimensional channels of CPL-1

The adsorption enhancement effect of multiple attractive interactions is attributed to the confronting and neighboring pore walls; this is characteristic of the nanometer-sized space

of a micropore (pore size <2 nm) [55]. This adsorption enhancement effect is useful not only for its application with gas storage materials and heterogeneous catalysts, but also for the unique properties of confined molecules that are different from those of the bulk fluid. Although a number of microporous compounds have been synthesized and utilized for many applications, less attention has been devoted to the regularity of the pore structure and utilization of uniform nanosized space. We focus on guest adsorption in regular periodic channels whose dimension is similar to that of the guest molecules, and in this sense, the CPL-1 would be most favorable candidate to confine guest molecules and form specific assemblies because of the small channel dimensions with uniform structure.

Ultramicropore filling, also termed primary micropore filling [56,57], occurs at very low relative pressure (P/P_0): it is associated with enhanced adsorbent–adsorbate interaction and results in a significant distortion of the isotherm such as the case of chemisorption. Generally, distinct from chemisorption, the guest molecules are bound to specific adsorption sites via a chemical bond; physisorption is nonspecific adsorption without any specific binding sites. This is because the dispersion force, which dominates the physisorption, is not usually very sensitive to surface properties. Physisorbed guest molecules tend to form an incommensurate relationship between guest molecule and host structures, and adsorption saturation changes according to the size and volume of the guest molecules. However, when the pore dimension is comparable to that of the guest molecules, the difference of adsorption potential becomes very large and clear following the channel periodicity. As a result, we can recognize some unusual “chemisorption-like physisorption” isotherms in the CPL-1 whose saturation exhibits exact integral number per unit pore, indicative of the commensurate relationship between guest molecules and host structure.

Fig. 9 shows adsorption isotherms of Ar, CH₄, N₂, and O₂ at 77 K and CO₂ at 195 K on CPL-1 [47]. The isotherms display a steep rise in the low relative pressure region followed by a plateau. All of the adsorption isotherms can be categorized as isotherms of Type I [56], indicative of a typical physisorption process by the microporous compound. The low onset pres-

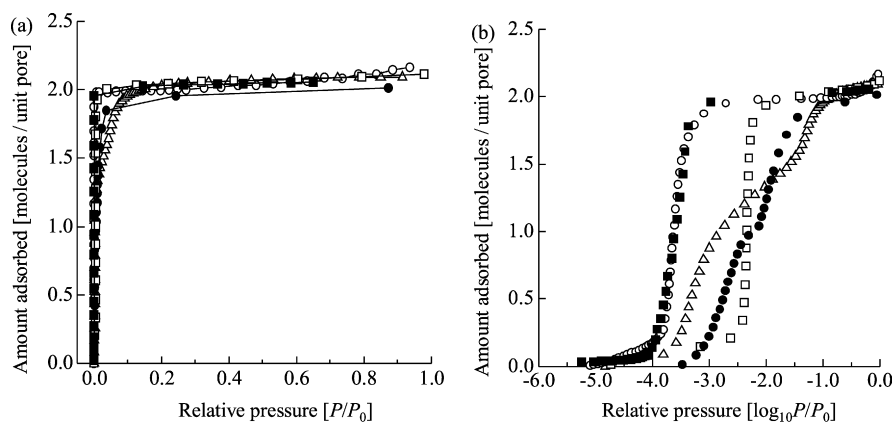


Fig. 9. Adsorption isotherms for N₂ (open circles), O₂ (solid squares), Ar (open squares), and CH₄ (solid circles) at 77 K and CO₂ (open triangles) at 195 K in the relative pressure range from 10^{−5} to 0.95, plotted against a relative pressure P/P_0 (a), and plotted against a logarithmic relative pressure $\log_{10} P/P_0$ (b). P_0 is the saturated vapor pressure for each adsorbate.

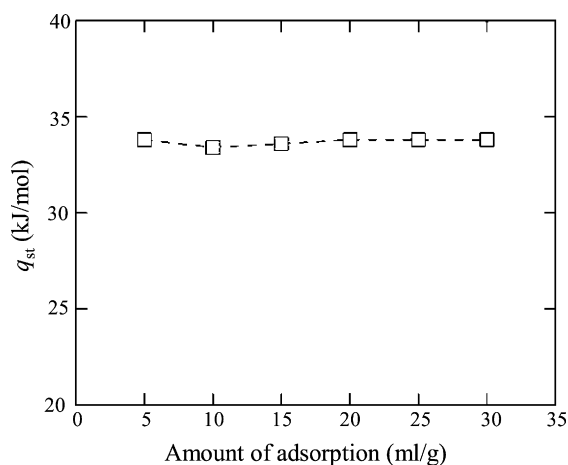


Fig. 10. Calculated isosteric heat of adsorption of CO_2 on CPL-1 plotted against amount of adsorption.

sure and sharp rise of the isotherm indicate that an extremely uniform and deep potential well forms in the ultramicropore of CPL-1. The value of isosteric heat of N_2 adsorption on CPL-1, which is estimated by Dubinin–Radushkevich equation [58], is greater than those of activated carbon fibers. Interestingly, in spite of the differences in the molecular volumes of the guest molecules (molecular volume of O_2 is only 68% of that of CO_2 , for example) the adsorption saturation of all the guest molecules in CPL-1 clearly shows a stoichiometry with just two guest molecules per unit pore. As illustrated in Fig. 10, the isosteric heat of adsorption for CO_2 is unchanged during the adsorption process, indicating that the CPL-1 adsorption sites are uniform. This, “chemisorption-like physisorption”, would be attributed to the confinement effect and commensurate adsorption of the well-regulated ultramicropore of CPL-1.

2.3. Formation of molecular arrays in CPL-1

Microporous coordination polymers are one of the most plausible candidates for the formation of specific molecular arrays because of their highly designable nature and pore homogeneity [5,44,59–61]. Sometimes, 1D arrays of solvent molecules result from the crystallization process [61–67]. O_2 and NO are among the smallest stable paramagnetic molecules under ambient conditions and have the potential to form new molecular-based magnetic and/or dielectric materials. However, we were not successful in many attempts to form 1D arrays of these paramagnetic gas molecules through confinement of the molecules in porous coordination polymers [68] or in microporous carbon materials [57,69]. Therefore, to form a regular assembly of these simple molecules in a nanochannel, it is important that we use not only the strong confinement effect of nanospace but also the commensurability between the host structure and guest molecule mentioned above, the amount adsorbed in each unit pore of CPL-1 shows precisely integral value [46,47]. This commensurate adsorption clearly indicates the formation of molecular arrays in the one-dimensional channel of CPL-1. Therefore, to elucidate

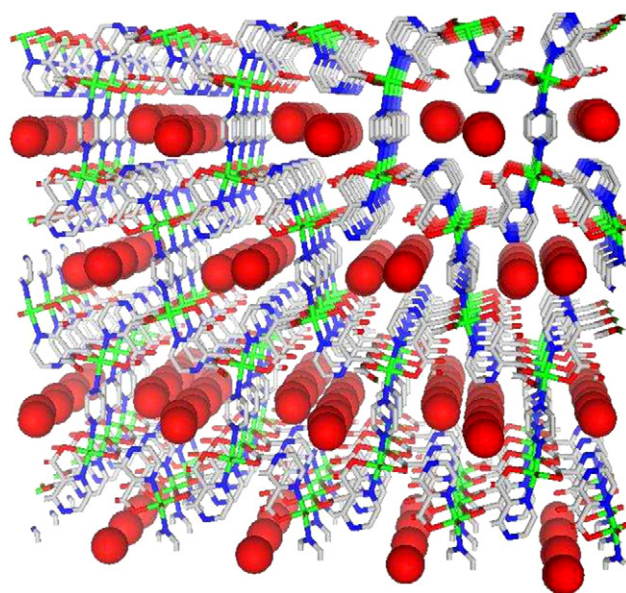


Fig. 11. The overall crystal structure of O_2 accommodated CPL-1. The framework and O_2 molecules are represented by stick and van der Waals surface models, respectively.

the structure of the adsorbed molecules, we first performed *in situ* X-ray powder diffraction (XRPD) measurements for CPL-1 accommodating O_2 molecules, and succeeded in determining a 1D ladder molecular array structure of O_2 . Direct observation of guest molecules accommodated in porous materials by X-ray and neutron structural analysis is very useful to study guest adsorption phenomena [46–51,70–82]. The overall crystal structure and geometry of the O_2 molecules are represented in Fig. 11. Two O_2 molecules are aligned parallel to each other along the a -axis with an inclination of 11.8° , with an inter-molecular distance of $3.28(4)$ Å. This inter-molecular distance is close to the nearest distance in solid α - O_2 phase, whose close packed structure appears below 24 K. This result indicates that O_2 molecules adsorbed in nanochannels form van der Waals dimers, $(\text{O}_2)_2$. Each dimer aligns along the a -axis to form a 1D ladder-like structure. The X-ray structure analysis reveals that O_2 molecules are in the solid state rather than the liquid state even at 130 K under 80 kPa, which is much higher than the boiling point of bulk O_2 under atmospheric pressure, 54.4 K. This result is ascribed to the strong confinement effect of CPL-1. The magnetic susceptibility for adsorbed O_2 molecules approaches zero with decreasing temperature, which indicates a nonmagnetic ground state of the antiferromagnetic dimer $(\text{O}_2)_2$ (Fig. 12). In the Raman spectrum the O_2 stretching-vibration mode appears as a sharp peak at a higher energy than that of solid α - O_2 under atmospheric pressure and comparable to that of α - O_2 under 2 GPa [83]. Interestingly, even under lower pressure than the saturated vapor pressure, the densities of the adsorbed phases of O_2 were much greater than those of the corresponding bulk liquid phases. This indicates that the adsorbed molecules are significantly different from the bulk state and, therefore, are considered to be a new state characteristic of molecules confined in the ultramicropore of CPL-1.

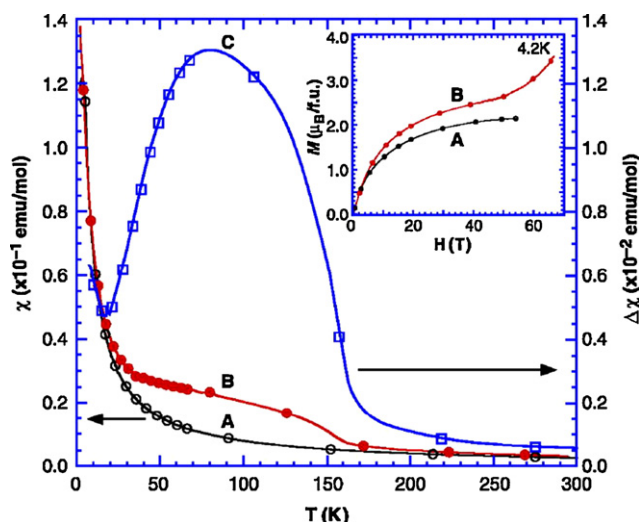


Fig. 12. Temperature dependence of the susceptibility of (A) CPL-1 and (B) CPL-1 with O_2 molecules, and (C) the differences between (A) and (B), correspond to the contribution from adsorbed O_2 molecules. (Inset) High-field magnetization process of (A) CPL-1 and (B) with O_2 molecules, χ , susceptibility; M , magnetization; μ_B , Bohr magneton; f.u., formula unit; H , magnetic field; T , temperature (figure was reproduced from Ref. [46], with permission of the copyright holders).

2.4. Molecular arrays of different shaped guest molecules in CPL-1

The structure of other simple guest molecules such as N_2 , Ar, and CH_4 accommodated in the CPL-1 could also be determined by X-ray crystallography. Hereafter, a guest adsorbed CPL-1 is denoted as CPL-1 \supset G (G = H_2O , O_2 , N_2 , Ar, and CH_4). These small molecules each possess a different size, shape, dipole moment, electric quadrupole moment, and magnetic moment (for example only the O_2 molecule has a magnetic moment, $S = 1$), which operate on the interaction force between adsorbed molecules and/or the pore walls.

Because the van der Waals interaction that dominates the physisorption process is a nonspecific interaction, the pore surface geometry such as size and shape can be essential for physisorption in an ultramicropore; this pore surface can be defined as a possible surface for a sphere of diameter 3.0 Å as it rolls over the surface of the channel in CPL-1. The pore surface is shown in Fig. 13, together with confined guest molecules. In the cases of Ar and CH_4 , two molecules can be accommodated in the unit pore of the channel similar to the case of O_2 . However, the molecular dimensions for Ar and CH_4 are different from that of O_2 , so that the molecular structure shows not a dimeric array but almost zigzag chain structure.

The most interesting feature is the difference of the pore surface. The pore surfaces of CPL-1 \supset Ar and CPL-1 \supset CH_4 are different from those of CPL-1 \supset O_2 . This is attributable to a sort of induced fit resulting from the framework flexibility of CPL-1 [45,84,85]. As is clearly illustrated in Fig. 13, the concavity and convexity of the channel with a periodicity of about 4.7 Å (namely, the length of the a -axis) provides pockets that are suitable in shape and size to confine guest molecules. This specific binding pocket should provide a significantly deep potential well along the channel direction.

2.5. Effect of periodic electric field of the pore

Although the pore surface geometry is a major factor to determine the shape of guest molecular assemblies in the nanochannel as mentioned above, the nature of the molecule–molecule and molecule–wall interactions is also important. A uniform channel structure provides a uniform periodic electric field in the nanospace, which can influence the structure of the guest molecular array in the channel. The N_2 and O_2 have almost same rod-like shape and the dimension of 2.991 and 2.930 Å, respectively, therefore, both guest molecules would form a similar arrangement in the channel, if the molecule–molecule and molecule–wall interaction is not considered. However, an appre-

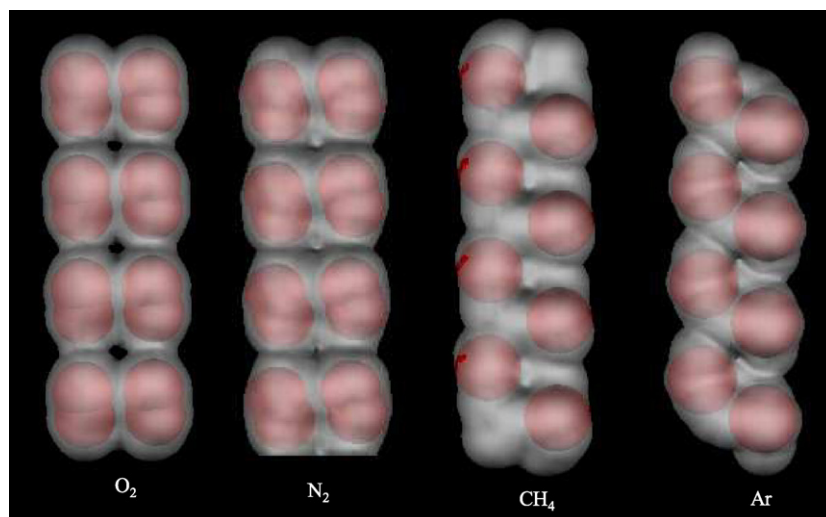


Fig. 13. Representation of confined guest molecules drawn by the space filling model and solvent-accessible pore surface, which is defined by the possible surface of a rolling sphere with a diameter 3.0 Å, along the channel directions (figure was reproduced from Ref. [47], with permission of the copyright holders).

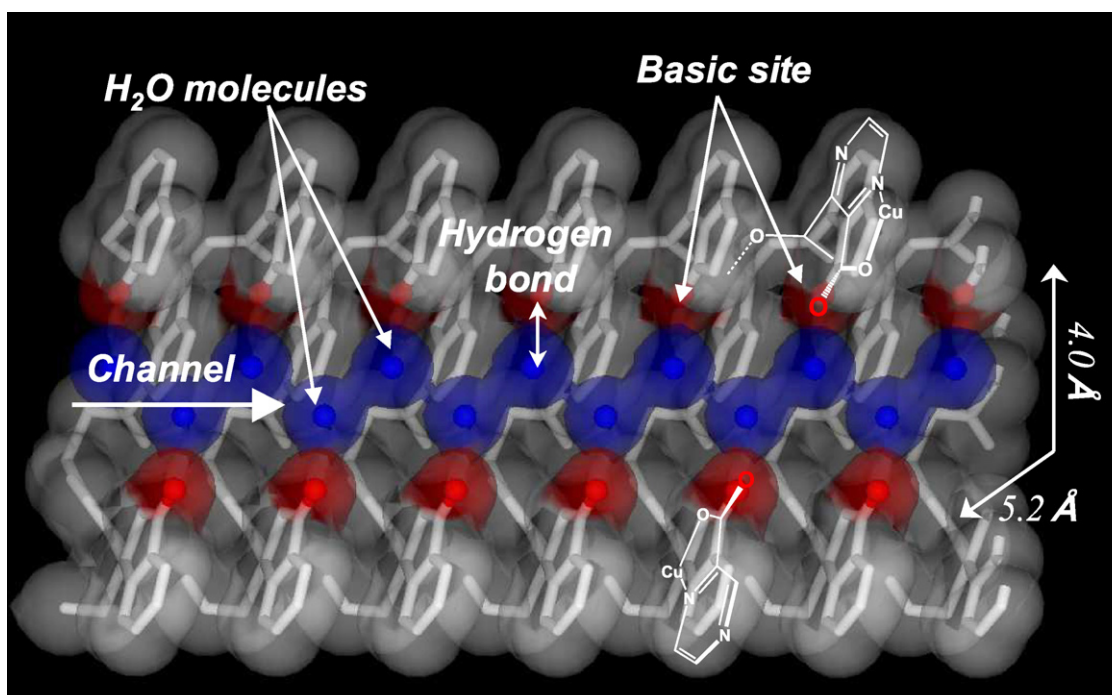


Fig. 14. The channel structure of as-synthesized CPL-1. One-dimensional array of water molecules supported by oxygen atoms on the pore surface in CPL-1, displayed by stick and van der Waals surface models.

ciable difference was observed in the orientation of the confined guest molecules. While O_2 molecules align parallel to the channel of CPL-1, N_2 molecules inclined against the channel direction to form offset van der Waals dimers. This difference would be attributed to the difference of the electric quadrupole moment; N_2 and O_2 molecules possess electric quadrupole moments of -1.33×10^{-40} and $-4.90 \times 10^{-40} \text{ C m}^2$, respectively [86].

2.6. Strong confinement effect enhanced by regularly aligned functional groups in nanochannel

One of the advantages of microporous coordination polymers, when compared with other microporous materials such as activated carbon, is designability, which provides a variety of surface properties based on organic ligands, affording unique functionalities on the channel surface. CPL-1 can show a high adsorption capability for specific molecules as a result of this prominent feature.

As-synthesized complex, $\text{CPL-1} \cdot 2\text{H}_2\text{O}$, shows an interesting aspect of the pore. The water molecules as guest molecules are connected to the oxygen atoms of the carboxylate groups on the pore surface in a one-to-one fashion, indicating that the oxygen atoms act as basic adsorption sites for guest molecules (Fig. 14). Accordingly, it is expected that the CPL-1 would exert an effective sorption ability on small molecules having acidic parts by deep van der Waals type potential energy well [87] and additional hydrogen-bonding interactions. The C_2H_2 molecule has a linear form with acidic hydrogen atoms at both ends ($\text{p}K_{\text{a}} = 25$). On the other hand, the CO_2 molecule has a rod-shaped form with the dimension of $3 \text{ \AA} \times 5 \text{ \AA}$, similar to that of C_2H_2 , however, it

has no acidic protons, therefore, we call attention to CPL-1 as a feasible adsorbate for the C_2H_2 molecule.

A marked difference in the C_2H_2 and CO_2 adsorption isotherms was observed. The adsorption isotherms of C_2H_2 show a steep rise in the very low-pressure region and reach saturation, whereas those of CO_2 show a gradual adsorption (Fig. 15). The saturation amount of C_2H_2 corresponds to just one molecule per unit pore. The maximum ratio of the adsorbed of C_2H_2 relative to that of CO_2 is 26.0 (at 1.1 kPa) at 270 K, indicating that CPL-1 accommodates C_2H_2 more preferentially than CO_2 . The isosteric heats (q_{st}) at the fractional filling ratio of 0.2

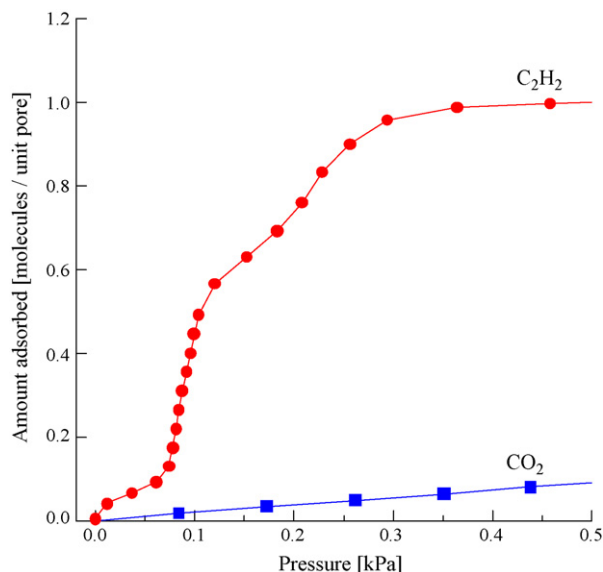


Fig. 15. The adsorption isotherms of C_2H_2 and CO_2 on CPL-1.

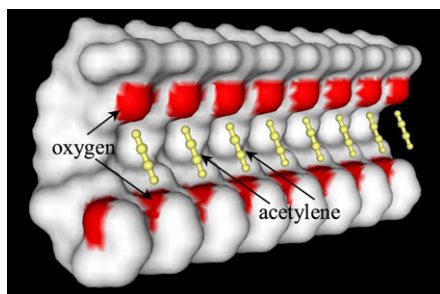


Fig. 16. The channel structure of acetylene accommodated CPL-1. The framework and acetylene molecules are displayed by solvent accessible surface and stick-and-ball model, respectively.

of C_2H_2 , 42.5 kJ/mol, is higher than that of CO_2 , 31.9 kJ/mol. These results indicate a higher enhancement in the interaction of C_2H_2 with CPL-1 than that of CO_2 .

In the acetylene accommodated structure, only one C_2H_2 molecule locates in the middle of the channels, whose stoichiometry is in good agreement with that of the adsorption measurement (Fig. 16). In the channel, the C_2H_2 molecules align along the a -axis with an inclination of 78.1° , and the inter-molecular distance is 4.8 Å, indicating that they are densely packed with a short inter-molecular distance while avoiding the close contact that induces an explosion. Each end of the C_2H_2 molecule is oriented to the two non-coordinated oxygen atoms on the pore wall. The distance between one hydrogen atom of C_2H_2 and the oxygen atom is found to be 2.2 Å, which is smaller

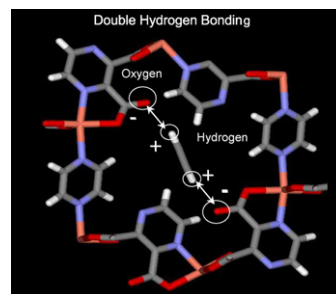


Fig. 17. The pore structure of acetylene accommodated CPL-1. The acetylene molecule located in the middle of pore is supported by two oxygen molecules via double hydrogen bonding.

than the sum of the van der Waals radius of hydrogen and oxygen atoms, 2.6 Å, indicative of the typical $O \cdots H-C$ hydrogen bond (Fig. 17). These interactions strongly fix the C_2H_2 molecule in every periodic unit pore and isolate the C_2H_2 in the 1D channel, which gives rise to the enhancement of the “confinement effect” and enables the stable accommodation.

The density of adsorbed C_2H_2 is estimated to be 0.434 g cm^{-3} ; this density value is equivalent to that of an extrapolated state of acetylene at 41 MPa at room temperature, and is 200 times larger than the value of the compression limit for the safe use of C_2H_2 at room temperature, 0.20 MPa [88] = 0.0021 g cm^{-3} [88].

The specific sorption ability of CPL-1 for C_2H_2 is ascribed to the proper and regular arrangement of the two basic oxygen

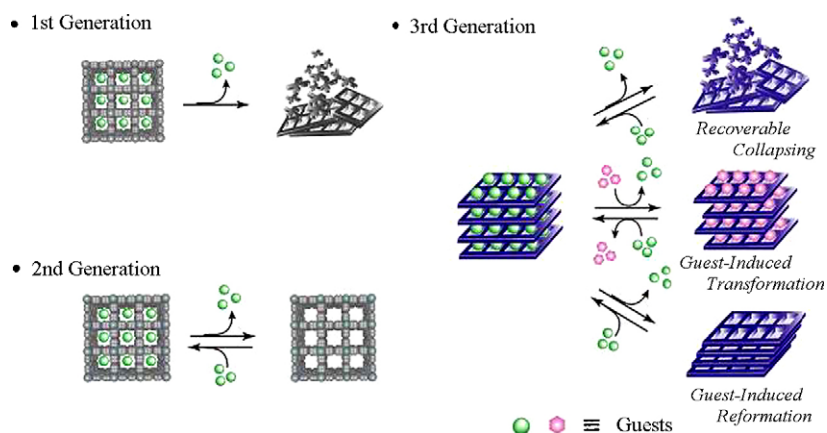


Fig. 18. Schematic view of first, second and third generation microporous coordination polymers.

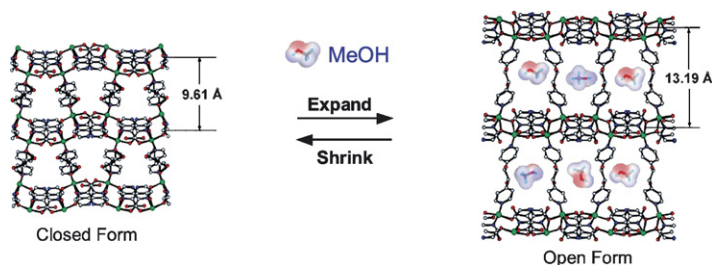


Fig. 19. Schematic view of pores expansion/shrinkage with methanol adsorption/desorption on CPL-6.

atom sites for an acetylene molecule. Usually, small molecules are adsorbed in a micropore, where van der Waals type potential operates efficiently. When functional sites are added to the pore, enhancement of the “confinement effect” is evidently observed. Furthermore, the stoichiometric guest incarceration is obtained with a commensurate structure of guest array with respect to that of host. According to these results, when the multiple specific interaction-sites are located at suitable positions on the regular micropore, the target molecule can be adsorbed in a specific fashion.

3. Flexible nature of coordination polymers

3.1. The guideline for flexible network

In the earliest days of porous coordination polymers, the rigid and robust open frameworks were an important target just as with zeolites [7]. As a result of the considerable activity, several coordination polymers were prepared with rigid open frameworks (Fig. 18), so-called “second generation” porous coordination polymers [20]. The $[\text{Cu}(\text{SiF}_6)(4,4'\text{-bpy})_2]_n$ [60] and $[\text{Zn}_4\text{O}(\text{BDC})_3]_n$ (BDC = benzenedicarboxylate anion) [89] were reported as a prototype in the context of “second generation” porous coordination polymer. In both compounds the rigid and divergent linkers allow articulation into a 3D framework, resulting in structures with higher apparent surface area and pore volume. Over the past few years many studies have reported the synthesis of thermally stable and robust 3D frameworks without guest molecules, in order to carry out porous functionalities [5,43,44,59,70,71,76,89–117].

The next challenge in this field is to develop a new stage from structural to functional, which could be associated with the dynamic aspects of the frameworks [4,118–122]. Dynamic pores could come from a sort of “soft” framework with bistability. Recent activities have provided several types of flexible porous coordination polymers and their dynamic functionalities [45,48,50,64,66,73,82,84,85,91,97,115,123–139] (Fig. 18) [20].

A guideline for rigid pores in coordination polymers is the use of stiff building units linked with strong chemical bonds such as coordination and/or covalent bond to form a 3D framework. On the other hand, dynamic pores are subject to another guideline for a sort of flexible framework, that is, building units (or motifs) with flexible moiety are linked with strong bonds, or, stiff building blocks (or motifs) are connected with weaker bonds. Another possible option is the combination of flexible building blocks (motifs) and weak linkages. The generation of a host framework that interacts with an exchangeable guest species in a switchable fashion has implications for the generation of previously undeveloped advanced materials with applications in areas such as molecular sensing. With the weak linkages, guest molecules readily change the bond orientation, distance, and cleavage. Even a weak interaction between guest and pore-wall molecules can induce a structural change because of a cooperative effect based on a large ensemble over an infinite framework. Coordination polymers form infinite networks, therefore extensive cooperativity would be expected between the molecules

throughout the crystal, such that rearrangements can occur in a well-concerted fashion, in order to maintain its macroscopic integrity. In this section, we will show three typical types of flexible coordination polymers with several significant examples below.

3.2. Bond elongation and shortening or cleavage and reformation

A structural transformation ascribed to stretching motions around the connector and/or linker results from bond formation/cleavage. The key factor in realizing such expandable frameworks is the utilization of weak interactions, such as hydrogen bonds [113], semicoordination, and the elongated coordination of Jahn–Teller distortions [48].

A hysteretic adsorption and desorption profile accompanied by a transformation of the crystal structure is observed for $\{[\text{Cu}_2(\text{pzdc})_2(\text{dpyg})]\cdot 8\text{H}_2\text{O}\}_n$ (CPL-7), (dpyg = 1,2-di(4-pyridyl)-glycol), which has a 3D pillared-layer structure [45]. This compound shows a reversible crystal-to-crystal transformation on adsorption and desorption of H_2O or MeOH molecules. A precise structure-determination study by high-resolution synchrotron powder X-ray diffraction reveals contraction and re-expansion of the channels with the layer–layer separation varying between 9.6 and 13.2 Å during the process of desorption/adsorption of the guest molecules; the unit-cell volume decreases during the contraction by 27.9% (Fig. 19). This structural transformation is attributed to the cleavage/formation of the Cu^{II} -carboxylate bond.

3D frameworks of $\{[\text{Cu}(\text{AF}_6)(4,4'\text{-bpy})_2]\cdot x\text{H}_2\text{O}\}_n$ were transformed into 2D interpenetrating networks of $\{[\text{Cu}(4,4'\text{-bpy})_2(\text{H}_2\text{O})_2]\cdot \text{AF}_6\}_n$ (A = Si, Ge, and Ti) when immersed in H_2O solution [140,141]. To demonstrate the occurrence of this dynamic structural transformation in the solid state, 3D frameworks of $\{[\text{Cu}(\text{AF}_6)(4,4'\text{-bpy})_2]\cdot x\text{H}_2\text{O}\}_n$ were exposed to H_2O vapor for a few days. The same transformation into a 2D interpenetrating framework was observed, clearly indicating the solid-state conversion. This transformation causes not only the formation and cleavage of weak Cu–O (H_2O) and Cu–F (AF_6) bonds, but also the formation and cleavage of Cu–N ($4,4'\text{-bpy}$) bonds. An important role is often played by the elongated axial sites of Cu^{II} compounds. M^{II} -bis(acetylacetonato) (M = Cu, Zn, Ni) derivatives have characteristic inclusion phenomena [64,142,143].

The 3D porous coordination polymer $[\text{Cu}_2(\text{pzdc})_2(\text{bpy})]$ (CPL-2) can adsorb one benzene molecule in each pore, which is located in the middle of the channel [48]. Upon adsorption of the benzene, the pillared layer framework undergoes a structural deformation such that the channel cavities suit the benzene molecules very well, resulting in appreciable differences in channel shape with and without benzene. The channel without benzene has nearly a rectangular shape of dimensions of $5.6 \text{ Å} \times 7.2 \text{ Å}$ whereas that with benzene is no longer a rectangular shape but a “Z” letter-shape (Fig. 20). Interestingly, in the absence of benzene, the geometry around the copper ion is square pyramidal, while that with benzene shows a square planar form, indicating the cleavage and reforming of the apical Cu–O

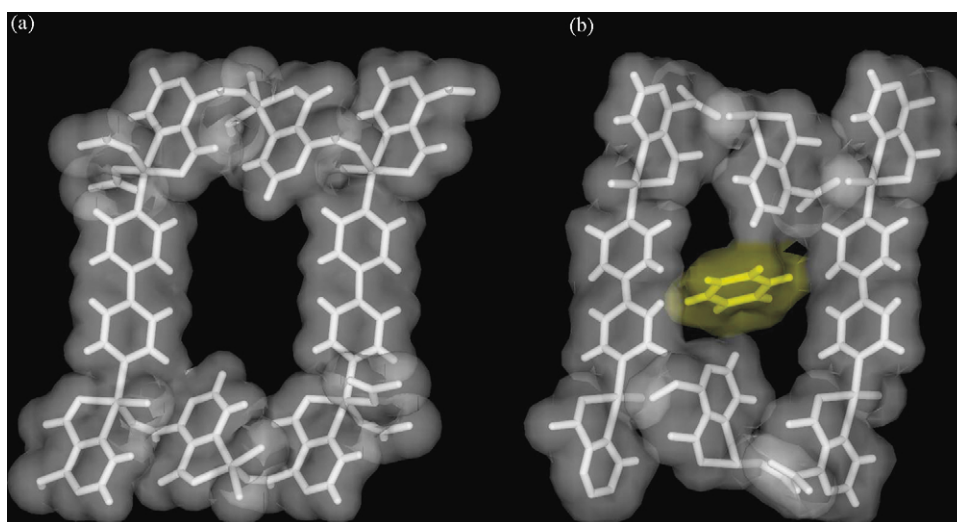


Fig. 20. Representation of the pore structures of (a) CPL-2 without guest molecule and (b) CPL-2 with benzene molecule. Both of views are displayed by stick and van der Waals surface models (figure was reproduced from Ref. [48], with permission of the copyright holders).

bond. Eventually, the deformation produces a large contact area to the benzene plane.

The $\{[M_2(4,4'\text{-bpy})_3(\text{NO}_3)_4] \cdot x\text{H}_2\text{O}\}_n$ ($M = \text{Co}$, $x = 4$; Ni , $x = 4$; Zn , $x = 2$) frameworks, which are best described as tongue-and-groove (bilayer) structures, have been synthesized and their gas-adsorption properties investigated at ambient temperature under higher pressure [43]. In particular the detailed sorption properties and structural flexibility of $[\text{Ni}_2(4,4'\text{-bpy})_3(\text{NO}_3)_4]$, were investigated [129,135]. $[\text{Ni}_2(4,4'\text{-bpy})_3(\text{NO}_3)_4]$ contains linear chains of bpy bridging metal centers, in turn connected by T-shaped bpy coordination at the metal into pairs. These pairs are aligned parallel to each other in A (which is templated by methanol) and perpendicular in B (ethanol-templated), giving maximum pore cavity dimensions of 8.3 Å. The cavities are connected by narrower windows, but the dynamics of the bridging bpy molecules confer sufficient space on the framework to

allow adsorbed species which appear oversized from the static view of the structure to pass through the windows and access the pores. Given the close relationship between the two structural types, possible mechanisms for interconversion involving minimal bond breakage can be proposed, which rely on the lability and reversibility of coordinate bond formation (Fig. 21) [4]. The hydrogen adsorption and desorption isotherms on B and A showed unprecedented hysteretic profiles, related to the dynamic opening of the “windows” between pores. This behavior has the potential ability to store H_2 at lower pressures [91].

Hydrogen bonds in the networks would play an important role in realizing “amorphous-to-crystal” transformation [113,144]. The amide group can serve as a hydrogen bonding site; H acceptor ($-\text{NH}-$) and receptor ($-\text{CO}-$) in a space surrounded by a framework. In $\{[\text{Co}(\text{NCS})_2(4\text{-peia})_2] \cdot 4\text{Me}_2\text{CO}\}_n$ ($4\text{-peia} = N\text{-(2-Pyridin-4-yl-ethyl)-isonicotinamide}$), the cobalt

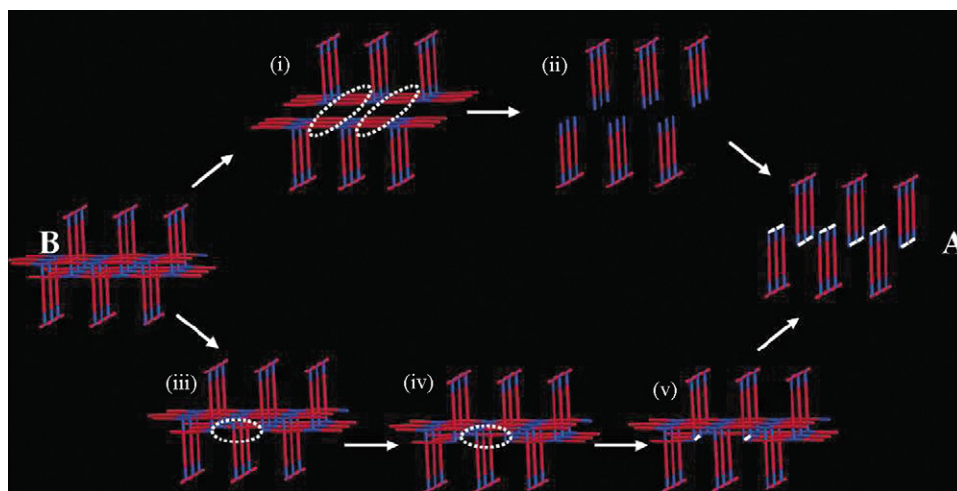


Fig. 21. Transformation from the B to the A structure of $\text{Ni}_2(\text{bpy})_3(\text{NO}_3)_4$ is possible via (i) separation of the bilayers, (ii) breaking 1/3 of the Ni–N bonds, or (iii) breaking both Ni–N bonds at two parallel bpy molecules then rotating the Ni–N bond direction of both by 90° (v) to form a ladder defect of A within B (figure was reproduced from Ref. [4], with permission of the copyright holders).

ions are linked by 4-peia to form a 2D layer composed of a square grid motif with the dimension of $15.8 \text{ \AA} \times 15.8 \text{ \AA}$ [145]. The hydrogen-bonding links of the $\text{NH} \cdots \text{O}=\text{C}(\text{N} \cdots \text{O})=2.780(7) \text{ \AA}$ groups between the adjacent layers create a complementary-amide binding network. A channel with the dimension of $4.4 \text{ \AA} \times 4.4 \text{ \AA}$ is observed, where acetone molecules are accommodated with no significant interaction. The framework cannot withstand a high level of stress or an extensive loss of the guest, resulting in an amorphous form. The 2D motif does not collapse, and the amorphous form is attributed to the random layer slip against the neighboring layers accompanying the deformation of the grid framework. Interestingly, upon exposure to acetone vapor, the original crystal structure is recovered completely, with hydrogen bonds among the layers effectively worked reconnected.

3.3. Sponge-like structural transformation

The structure of MIL-53 $\{[\text{M}(\text{OH})(1,4\text{-BDC})]\cdot\text{H}_2\text{O}\}_n$ ($\text{M} = \text{Al}^{3+}$, Cr^{3+}) exhibits a 3D structure built up from Cr(III) or Al(III) octahedra and BDC ions, creating a 3D framework with a 1D pore channel system. The MIL-53 solids exhibit a large breathing phenomenon upon hydration and dehydration [92,133,146]. In addition, the MIL-53 shows an unusual step in the CO_2 adsorption isotherm which may be due to the presence of interactions between the CO_2 molecules and the OH groups [147]. A three-dimensional iron(III) fumarate framework MIL-88, $\text{Fe}_3^{\text{III}}\text{O}(\text{CH}_3\text{OH})_3\{-\text{O}_2\text{C}-\text{C}_2\text{H}_2-\text{CO}_2-\}_3\cdot\{-\text{O}_2\text{C}-\text{CH}_3\}\cdot 4.5\text{CH}_3\text{OH}$, exhibits an exceptionally large swelling structural transformation, almost doubling its cell volume [148] (Fig. 22).

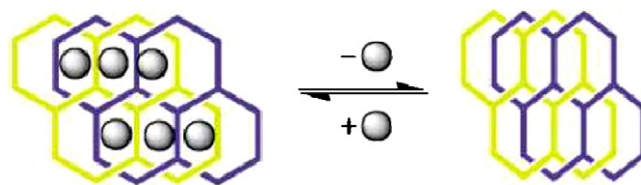


Fig. 23. Schematic representation of the contraction or expansion of the 3D network on the removal or addition of guest molecules, respectively (figure was reproduced from Ref. [123], with permission of the copyright holders).

A doubly interpenetrated network is synthesized by using tpt (2,4,6-tris(4-pyridyl)triazine) and ZnI (Fig. 23) [123]. Despite this interlocking of the networks, 60% of the unit-cell volume is occupied by the guest molecules, nitrobenzene. The unit-cell volume of this framework shrinks by 23% when the guest molecules are removed and swells when they are returned. This sponge-like swelling and contraction is attributed to rotation of the Zn–N coordination bonds. The bilayer open framework structure $[\text{Ni}_2(\text{C}_{26}\text{H}_{52}\text{N}_{10})]_3(1,3,5\text{-btc})_4$ (btc = benzene tricarboxylate), which is constructed from the dinickel(II) bis-macrocyclic complex $[\text{Ni}_2(\text{C}_{26}\text{H}_{52}\text{N}_{10})]$ and $1,3,5\text{-btc}^{3-}$, has 3D channels which are filled with 36 water and six pyridine guest molecules [126]. The channel walls created on the side of the bilayer are made of *p*-Xylyl pillars. By removal of all the pyridine and 32 water molecules, a sponge-like crystal structural transformation occurs which is due to the tilting of the pillars, which in turn is attributed to the rotation of the C–C bonds. The transformation takes place without breaking the crystallinity.

Flexible and dynamic microporous coordination polymers based on interdigitation, $[\text{Cu}_2(\text{dhbc})_2(4,4'\text{-bpy})]_n$ (CPL-p1), (dhbc = 2,5-dihydroxybenzoic anion) [85], and interpenetra-

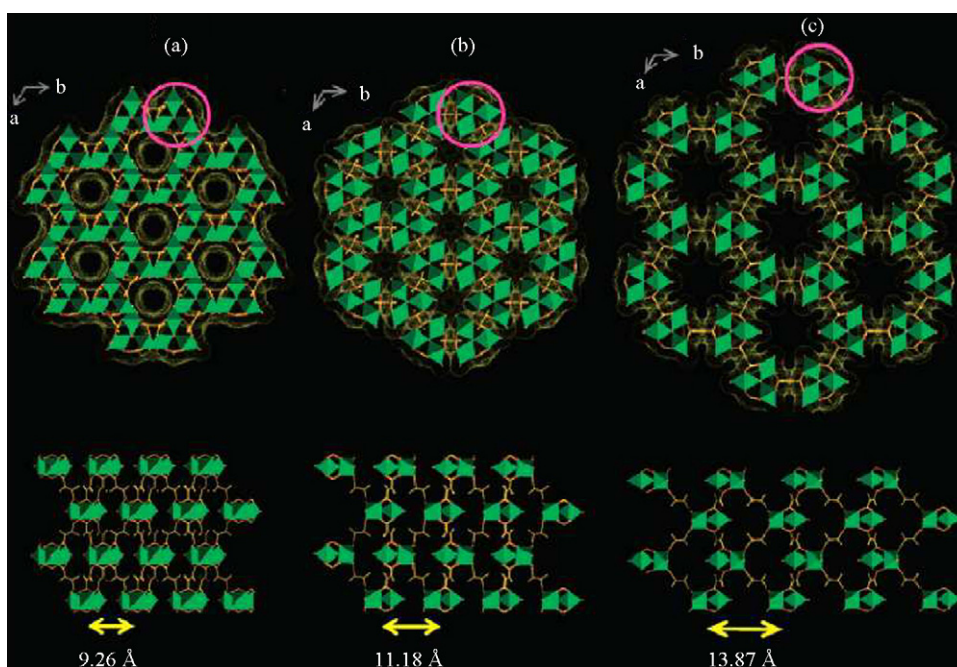


Fig. 22. Simulated crystal structures of the MIL-88 framework in its contracted (a), as-synthesized (b), and open (c) forms. It is noteworthy that the *a* cell parameter increases gradually from one structure to the next, as a direct measure of distance between the inorganic trimeric units and of the amplitude of the swelling (figure was reproduced from Ref. [148], with permission of the copyright holders).

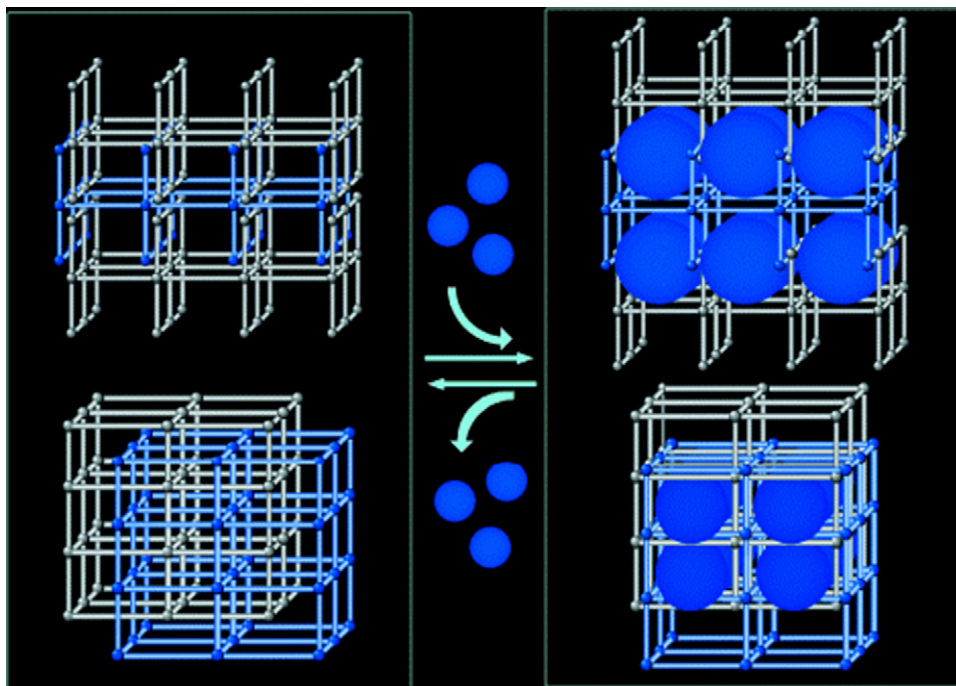


Fig. 24. Schematic representation of dynamic frameworks. Above: interdigitated framework of layers whose gap depends on the guest molecules. Below: Interpenetrated framework whose interunit space depends on the guest molecules (figure was reproduced from Ref. [85], with permission of the copyright holders).

tion, $[\text{Cu}(\text{1,4-BDC})(4,4'\text{-bpy})_{0.5}]_n$ (CPL-v1), (Fig. 24) [85,97], have been synthesized and characterized. The structure of CPL-p1, contains a 2D interdigitated F motif, and CPL-v1 gives a 3D interpenetrated motif. XRPD studies show that CPL-p1 undergoes a drastic crystal transformation triggered by desorption of included water and guest adsorption. A detailed structure investigation by synchrotron powder X-ray diffraction shows a cell-parameter change on dehydration from $a = 8.167(4)$, $b = 11.094(8)$, $c = 15.863(2)$ Å, and $\beta = 99.703(4)^\circ$ to $a = 8.119(4)$, $b = 11.991(6)$, $c = 11.171(14)$ Å, and $\beta = 106.27(2)^\circ$, which corresponds to a cell-volume contraction of 27%. This structural transformation of CPL-p1, especially the change of the length of the c -axis, is accompanied by a shrinking of the layer gap, which is attributed to a glide motion of the two π -stack ring moieties, dhbc, which results in a decrease in the channel cross-section. Interestingly, structural re-expansion was observed (confirmed by XRPD) when the compound is exposed to N_2 vapor below 160 K. This contraction and expansion behavior could be repeated many times. CPL-p1 shows characteristic hysteretic adsorption isotherms which have gate-opening and -closing pressures for CO_2 vapor and various super critical gases (CH_4 , O_2 and N_2). This behavior was observed on measuring the temperature dependence of the adsorption and desorption isotherms. This characteristic adsorption behavior should be attributed to crystal structure expansion and contraction triggered by gas adsorption and desorption. CPL-v1 also shows similar adsorption isotherms, which result from a glide motion of interpenetrated networks.

Kanoh et al. showed a gate opening type adsorption phenomenon with sponge-like structural transformation in the 2D layered open framework $[\text{Cu}(\text{BF}_4)_2(4,4'\text{-bpy})_2]$ (Fig. 25). Interestingly, the interlayer distance changes from 0.46 to 0.68 nm

with CO_2 gas adsorption, indicating an expansion of the inter-layer structure. This change corresponds to a 49% increase of the interlayer distance. The expansion of the 2D sheet structure concomitantly induces the formation of many open pores,

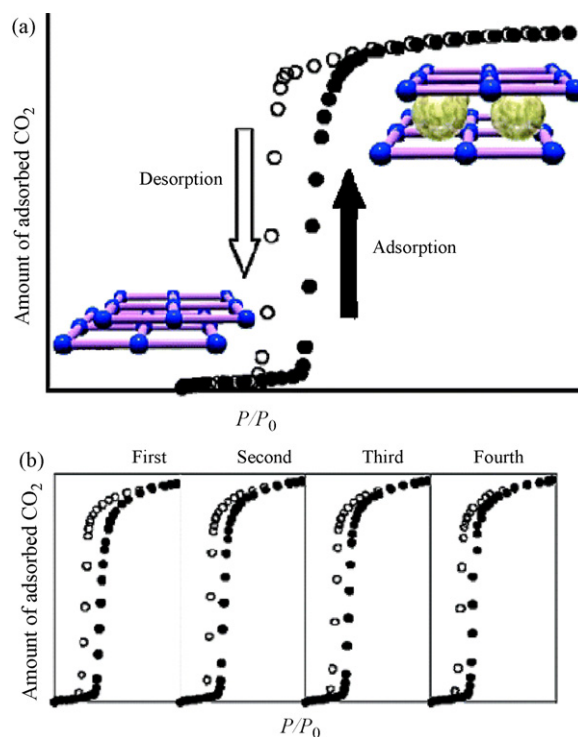


Fig. 25. Schematic representation of the gate adsorption phenomenon of CO_2 associated with structural transformation and clathrate formation (a) and the successive reproducibility over four cycles (b) (figure was reproduced from Ref. [150], with permission of the copyright holders).

and thus CO₂ molecules (minimum dimension: 0.28 nm) can be accommodated in the micropores of the framework [149,150].

Anion-exchange property is one of the representative functions of coordination polymers. After the first report of anion-exchange properties in 1990 [39], a number of reports showing this function have been reported [102,131,135,140,151–163]. Very recently, it was shown that anion exchange in the flexible framework could control gas-adsorption properties [164]. A bimodal microporous twofold interpenetrated network $\{[\text{Ni}(\text{bpe})_2(\text{N}(\text{CN})_2)](\text{N}(\text{CN})_2) \cdot (5\text{H}_2\text{O})\}_n$ (bpe = 1,2-bis(4-pyridyl)ethane), has two types of channels for anionic $\text{N}(\text{CN})_2^-$ (dicyanamide) and neutral water molecules, respectively. The dehydrated framework shows specific anion exchange of free $\text{N}(\text{CN})_2^-$ for the smaller N_3^- anions. The result of CO₂ adsorption measurement of the N_3^- -exchanged framework shows that about 10 ml/g more CO₂ is adsorbed compared with the as-synthesized $\text{N}(\text{CN})_2^-$ anion compound. This is possible because the N_3^- anion is smaller than the $\text{N}(\text{CN})_2^-$ anion, which leads to a dislocation of the mutual positions of the two interpenetrated frameworks due to sliding, and this results in an increase in channel size or more space to accommodate a larger number of CO₂ molecules.

3.4. Rotational motion of aromatic rings

Recent studies have explored the rotational motion of the aromatic rings, which very often exist in the structure, showing that they can afford new flexible features in the porous coordination polymers [78,79,81,82,136,139,165].

A coordination polymer composed of rhodium(II) benzoate and pyrazine $[\text{Rh}_2^{\text{II}}(\text{O}_2\text{CPh})_4(\text{pyz})]_n$ (**1**) shows an interesting rotational motion in the structure upon the inclusion of light gas molecules such as O₂, CH₄ and CO₂ (Fig. 26) [78,79,81,82,166,167]. The component chains found in crystals of **1** adopt a perfectly linear geometry with the chain skeleton bridged by the pyrazine group in the axial direction of the well-known paddle wheel type of dinuclear rhodium benzoate. The original framework has no channel structures sufficient to hold guest molecules, although there are empty cages with dimensions of 9 Å × 4 Å × 3 Å, with narrow gaps of approximately 1 Å found at their four corners, which are formed by the benzene rings of benzoate moieties arranged parallel to the chain vector. However, on cooling samples in a CO₂ atmosphere, the crystal underwent a phase transition to a new structure, generating one-dimensional (1D) channels. The cages are transformed into channels by a slippage of the chain skeletons along the chain vector; the benzene ring tilts 9° away from the chain vector.

Kubota et al. reported that the rotational motion of the pyrazine ring in the framework has an important role for the effective accommodation of acetylene in the CPL-1 host (Fig. 27) [50]. As mentioned above, the acetylene molecules are strongly confined in CPL-1 supported by double hydrogen bonding in the acetylene-saturated phase (phase S). However, when only 0.7 acetylene molecules are introduced to CPL-1 in each pore, a different intermediate structure (phase M) appears. Namely, the CPL-1 host framework undergoes the following structural transformation; guest free (initial) phase I, then the

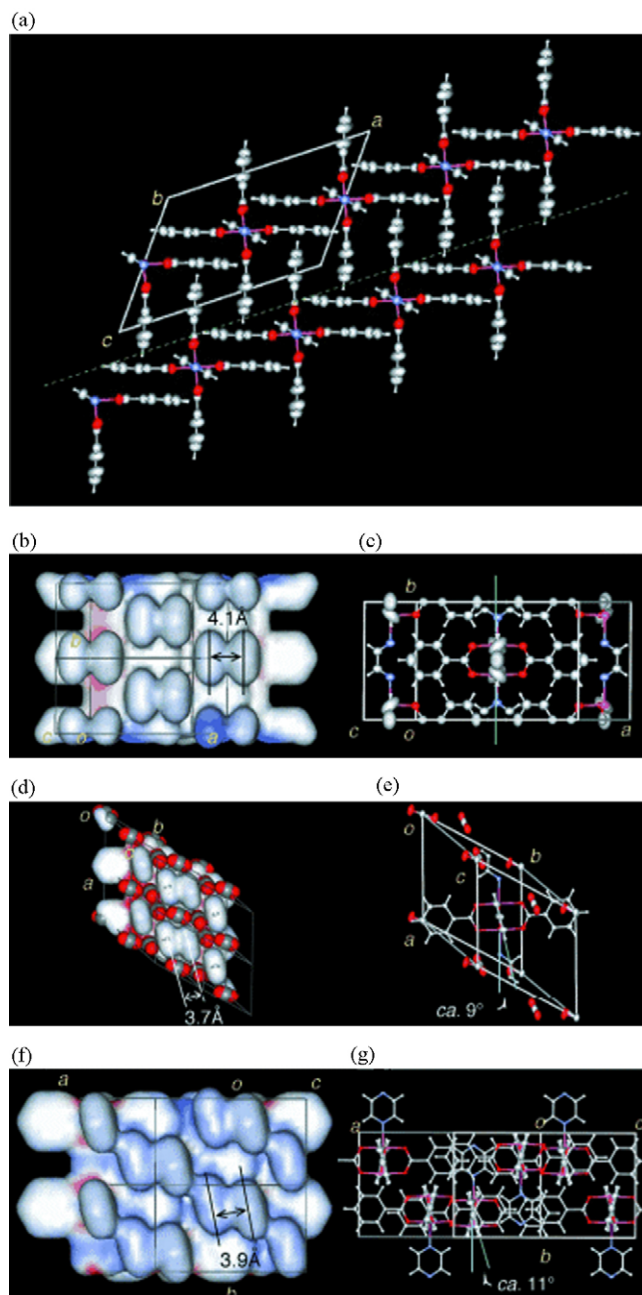


Fig. 26. Views of crystal $[\text{Rh}_2^{\text{II}}(\text{O}_2\text{CPh})_4(\text{pyz})]_n$: (a) view along the chain vector showing thermal ellipsoids for the crystal structure in CO₂ atmosphere at 20 °C; (b) surface view along the dashed cross-section of (a); (c) the corresponding ellipsoidal view; (d) surface view of the CO₂-inclusion state at -180 °C; (e) the corresponding ellipsoidal view; (f) surface view of the crystal under conditions where CO₂ was absent at -180 °C; (g) the corresponding ellipsoidal view. All ellipsoidal views are shown at 50% probability (figure was reproduced from Ref. [82], with permission of the copyright holders).

intermediate phase M, finally the phase S appears. During the structural transformation, a slight rotation of the pillar pyrazine ring ligands and shearing of the crystal lattice in the channel direction indicate a flexible transformation for efficient guest accommodation. Subsequently, phase M changes to phase S with a slight rotation of the acetylene molecules, and then hydrogen bonds are formed with the two uncoordinated oxygen atoms. With this change, there is now sufficient space for the pyrazine

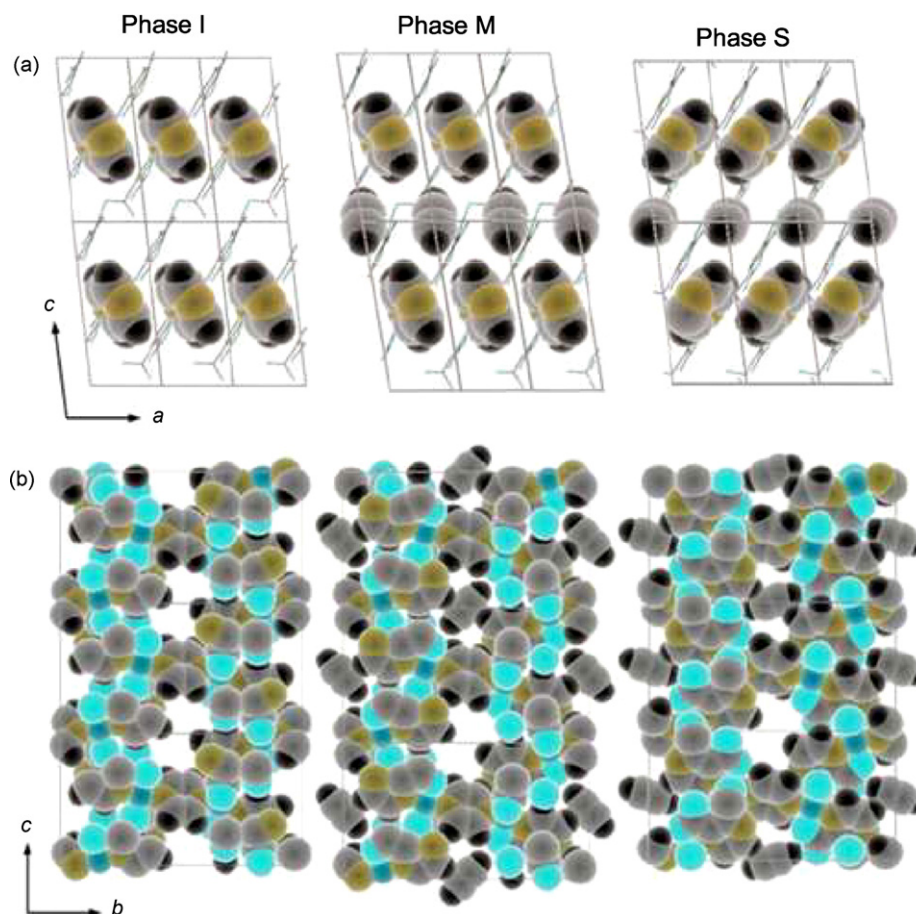


Fig. 27. Crystal structures of CPL-1 with adsorbed acetylene: (a) side views of the nanochannels. Pillar molecules (pyrazine) and adsorbed acetylene molecules are shown as CPK models. Otherwise, they are connected by lines; (b) views from the nanochannel direction as CPK model. Adsorbed acetylene molecules are omitted from lower central pore in phases M and S (figure was reproduced from Ref. [50], with permission of the copyright holders).

ring to rotate. The hydrogen bond between the hydrogen atom of pyrazine and the neighboring oxygen atom in the framework is associated with rotation of the pyrazine rings. This results in rather a different orientation of pyrazine in phase S from that in phases I and M. Shearing of the lattice also occurs again to induce more efficient guest accommodation. In the phase change from phase M to S, the unit-cell volume decreases, whereby the lattice parameter c contracts due to the change in orientation of the acetylene molecule forming double hydrogen bonds with two oxygen atoms on the pore wall. However, rotation of the pillar ligand makes space without changing the pore volume significantly. At the same time, the change in size and shape of the nanochannel causes more acetylene loading to reach adsorption saturation.

Desolvation of the single crystal of $[\text{Zn}_4\text{O}(\text{NTB})_2] \cdot 3\text{DEF} \cdot \text{EtOH}$ (DEF = *N,N'*-diethylformamide, NTB = 4,4',4''-nitrilotrisbenzoate) afford the apohost $[\text{Zn}_4\text{O}(\text{NTB})_2]$ without losing crystallinity [136]. Upon desolvation, the Zn_4O cluster and NTB^{3-} units undergo significant positional and rotational rearrangements by keeping the original positions of the central oxygen atom and the nitrogen atom of one of the two independent NTB^{3-} units. In particular, three phenyl rings around the Zn_4O cluster are rotated with respect to the C–C axes, and

the cluster unit also undergoes rotational motion. These rotations of the phenylene rings are triggered by π – π interaction. When the free space is produced in the crystal by guest solvent removal, the molecular components undergo significant rearrangements mainly with rotational motion to induce the stronger edge-to-face π – π interactions. To maintain the original 3D integrity, extensive cooperative motion occurs throughout the crystal (Fig. 28).

In the framework of $[\text{Zn}_2(1,4\text{-ndc})_2(\text{dabco})]_n$ (1,4-ndc = 1,4-naphthalenedicarboxylate, dabco = 1,4-diazabicyclo[2,2,2]octane), paddle-wheel Zn^{2+} dimers are linked by 1,4-ndc ions and dabco molecules, resulting in formation of rectangular channels with the cross-section of $5.7 \text{ \AA} \times 5.7 \text{ \AA}$ [139,168]. At 296 K, the naphthalene ring of the dicarboxylate ion is disordered over four positions, indicative of enough void space in the framework for rotation about the naphthalene ring (Fig. 29). The ^2H NMR study for the deuterated-framework revealed the naphthalene ring can rotate around the dicarboxylate C–C axis in a four-site flip motion. In addition, after the adsorption of benzene, the NMR spectrum of the framework is drastically different from that of the anhydrous one, indicating a decrease of the rotational motion, because the guest molecules interfere with the free rotation of the naphthalene rings in the open framework [139].

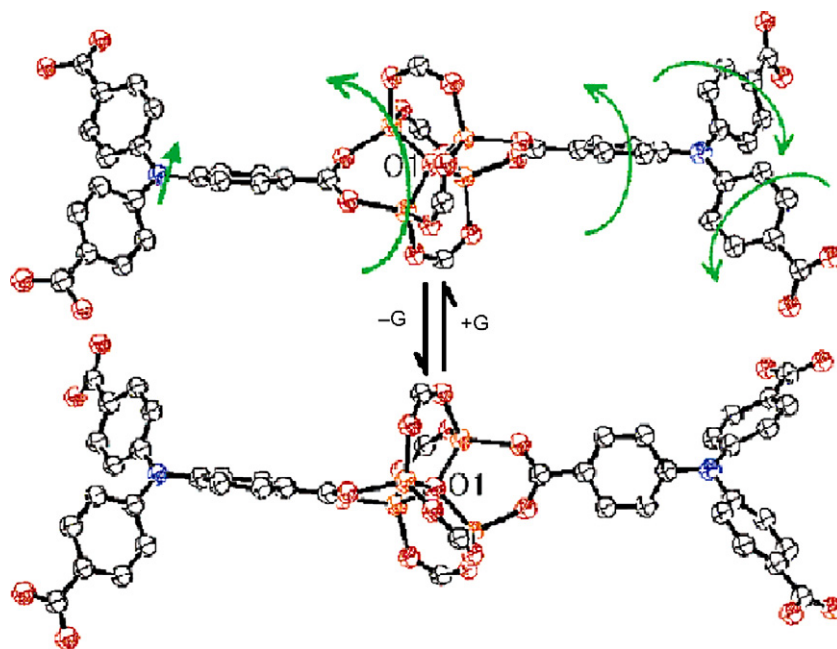


Fig. 28. Rearrangements of the $[\text{Zn}_4\text{O}(\text{NTB})_2]$ framework components upon guest removal and rebinding. Thermal ellipsoids are drawn with 50% probability (figure was reproduced from Ref. [136], with permission of the copyright holders).

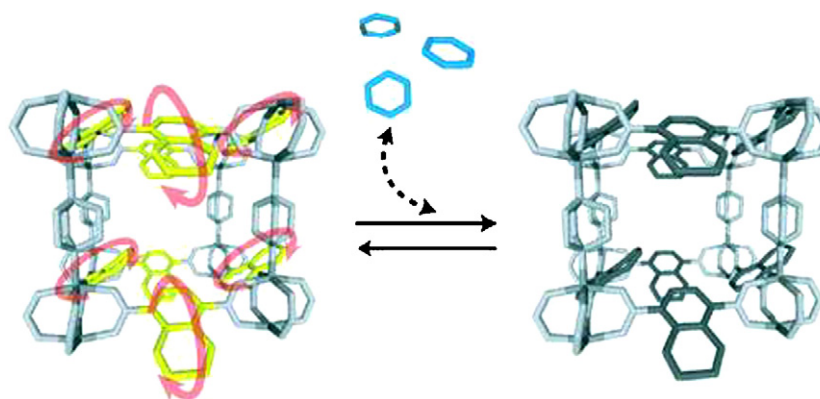


Fig. 29. (a) Schematic view of the guest-induced reversible rotation in the framework $[\text{Zn}_2(1,4\text{-ndc})_2(\text{dabco})]_n$ (figure was reproduced from Ref. [139], with permission of the copyright holders).

4. Perspectives

As shown above, molecules and atoms confined in nanospace exhibit interesting properties that are not observed in the corresponding bulk state. To develop the chemistry and physics of confined molecules and atoms in the low-dimensional nanospace, precise control and tuning of (1) pore size and (2) shape and periodicity of a unit that is well-suited for a target guest is of significance. For this purpose, possible candidates for mesopore and micropore regions are mesoporous silicas (MCM and FSM) and coordination polymers, respectively. As for treating small di- and triatomic molecules, compounds having micropores are relevant for their ordered array because a well-suited frame is effective for trapping and arranging the molecules in a channel. It is useful to take advantage not only of the size and shape but also the homogeneity of nanospaces in

coordination polymers. Therefore, chemists and physicists could collaborate with each other, finding various novel properties and producing new materials by using porous coordination polymers. This is a new type of field available for gases, called “gas molecule-accumulation science”. In particular, “gas molecule-accumulation science” is important because most of the gases, H_2 , O_2 , CO , NO , CO_2 , and CH_4 are associated with important issues of environment, energy, life, and their related materials. A large number of porous coordination polymers have been reported so far, forming a large database, which can be categorized into (1) structures and (2) functions. On this basis, we could search a porous structure most suitable for properties on demand. For this purpose, efforts are required to catalog and categorize all the compounds and to prepare a usable database. The following are categories for future porous coordination polymers.

4.1. Cooperative properties with functional framework and guest molecules

Actually, porous coordination polymers, whatever their structural dimensionality, possess two inherent characteristics; a porous framework and a guest molecule. Not only the properties of functional guests but those of porous frameworks (nonlinear optical properties, conductivity, magnetism, spin-crossover, chromism, and fluorescent properties) have been hitherto independently studied. Several examples of properties that framework functionalities change by inclusion and removal of guest molecules, which induce the change of the environment of metal centers, are also known. In these systems, guest molecules have no function in themselves. The next step is to research cooperative properties [23] with functional frameworks and guest molecules. In a restricted micropore, unprecedented cooperative properties are expected. They are so-called third generation compounds [20].

4.2. Low-dimensional form—thin layer compounds

Researchers control the size, shape, and distribution of pores and will establish this engineering in the near future. However, even when they have nanosized channels or cavities, compounds are at least μm -sized microcrystals, insoluble in any solvents, and therefore are hard to prepare in a thin layer form. Because of this, new methods to prepare a 2D sample are expected.

4.3. Mesoscale compounds

The next challenge in this field is at the mesoscale, with the aim of closing the gap between so-called top-down and bottom-up approaches to materials assembly. The ultimate goal is the ability to control the arrangement of channels, which means the formation of porous modules for various nanodevices. In order to do so, small nanocrystals are required, which can act as wells, wires, rods, and dots [169–172].

4.4. Introduction of anisotropy

The resolution of chiral frameworks for enantioselective sorption and asymmetric heterogeneous catalysis remains challenging and a mainly unexplored area. The use of chiral template molecules or the employment of enantiomerically pure organic linkers are the options for the preparation of the functional chiral frameworks [8,102,173].

4.5. Redox frameworks

Another exciting and undeveloped area is the systematic design and synthesis of redox-active porous frameworks, *i.e.*, oxidation and reduction of the overall framework can be performed by the guest molecules, without overall decomposition of the network. If a neutral open framework could be oxidized, it would include free counter anions in the channels or pores, and then it might be applied for anion-exchange materials and

also will affect the other properties, such as magnetism, *etc.* [73,115,174,175].

Acknowledgements

This work was supported by Grants-in-Aid for Scientific Research in a Priority Area “Chemistry of Coordination Space” (434) and a CREST/JST program from the Ministry of Education, Culture, Sports, Science, and Technology, Government of Japan.

References

- [1] J.-M. Lehn, *Supramolecular Chemistry*, VCH, 1995.
- [2] F. Schüth, K.S.W. Sing, J. Weitkamp, *Handbook of Porous Solids*, vol. 1, VCH, 2002.
- [3] D.W. Breck, *Zeolite Molecular Sieves*, Wiley & Sons, New York, 1984.
- [4] D. Bradshaw, J.B. Claridge, E.J. Cussen, T.J. Prior, M.J. Rosseinsky, *Acc. Chem. Res.* 38 (2005) 273.
- [5] G. Férey, C. Mellot-Draznieks, C. Serre, F. Millange, *Acc. Chem. Res.* 38 (2005) 217.
- [6] F. Schüth, K.S.W. Sing, J. Weitkamp, *Handbook of Porous Solids*, vol. 2, Wiley-VCH, Weinheim, 2002.
- [7] O.M. Yaghi, M. O’Keeffe, N.W. Ockwig, H.K. Chae, M. Eddaoudi, J. Kim, *Nature* 423 (2003) 705.
- [8] D. Bradshaw, T.J. Prior, E.J. Cussen, J.B. Claridge, M.J. Rosseinsky, *J. Am. Chem. Soc.* 126 (2004) 6106.
- [9] M. Eddaoudi, D.B. Moler, H. Li, B. Chen, T.M. Reineke, M. O’Keeffe, O.M. Yaghi, *Acc. Chem. Res.* 34 (2001) 319.
- [10] S. Kitagawa, R. Kitaura, S.-I. Noro, *Angew. Chem., Int. Ed. Engl.* 43 (2004) 2334.
- [11] C. Janiak, *Angew. Chem., Int. Ed. Engl.* 36 (1997) 1431.
- [12] S.R. Batten, R. Robson, *Angew. Chem., Int. Ed. Engl.* 37 (1998) 1460.
- [13] A.J. Blake, N.R. Champness, P. Hubberstey, W.-S. Li, M.A. Withersby, M. Schröer, *Coord. Chem. Rev.* 183 (1999) 117.
- [14] O.R. Evans, W. Lin, *Acc. Chem. Res.* 35 (2002) 511.
- [15] I. Goldberg, *Chem. Eur. J.* 6 (2000) 3863.
- [16] P.J. Hargman, D. Hargman, J. Zubietta, *Angew. Chem., Int. Ed. Engl.* 38 (1999) 2638.
- [17] A.N. Khlobystov, A.J. Blake, N.R. Champness, D.A. Lemenovskii, A.G. Majouga, N.V. Zyk, M. Schröer, *Coord. Chem. Rev.* 222 (2001) 155.
- [18] K. Kim, *Chem. Soc. Rev.* 31 (2002) 96.
- [19] S. Kitagawa, M. Munakata, *Trends Inorg. Chem.* 3 (1993) 437.
- [20] S. Kitagawa, M. Kondo, *Bull. Chem. Soc. Jpn.* 71 (1998) 1739.
- [21] S. Kitagawa, R. Kitaura, *Comments Inorg. Chem.* 23 (2002) 101.
- [22] S. Kitagawa, S. Kawata, *Coord. Chem. Rev.* 224 (2002) 11.
- [23] B. Moulton, M.J. Zaworotko, *Chem. Rev.* 101 (2001) 1629.
- [24] M. Munakata, *Adv. Inorg. Chem.* 46 (1998) 173.
- [25] H. Okawa, M. Ohba, *Bull. Chem. Soc. Jpn.* 75 (2002) 1191.
- [26] O.M. Yaghi, H. Li, C. Davis, D. Richardson, T.L. Groy, *Acc. Chem. Res.* 31 (1998) 474.
- [27] M.J. Zaworotko, *Chem. Soc. Rev.* (1994) 283.
- [28] M.J. Zaworotko, *Chem. Commun.* (2001) 1.
- [29] C. Janiak, *Dalton Trans.* (2003) 2781.
- [30] G.K.H. Shimizu, *J. Solid State Chem.* 178 (2005) 2519.
- [31] J.J. Vittal, *Coord. Chem. Rev.* 251 (2007) 1781.
- [32] R.M. Barrer, *Molecular Sieves*, American Chemical Society, Washington, DC, 1974.
- [33] R.E. Wilde, S.N. Ghosh, B.J. Marshall, *Inorg. Chem.* 9 (1970) 2512.
- [34] H.J. Buser, D. Schwarzenbach, W. Petter, A. Ludi, *Inorg. Chem.* 16 (1977) 2704.
- [35] K.R. Dunbar, R.A. Heintz, *Prog. Inorg. Chem.* 45 (1997) 283.
- [36] J.L. Atwood, J.E.D. Davies, D.D. MacNico, *Inclusion Compounds*, vol. 1, Academic Press, London, 1984.

- [37] J.L. Atwood, J.E.D. Davies, D.D. MacNico, *Inclusion Compounds*, vol. 5, Oxford Univ. Press, Oxford, 1991.
- [38] Y. Kinoshita, I. Matsubara, T. Higuchi, Y. Saito, *Bull. Chem. Soc. Jpn.* 32 (1959) 1221.
- [39] B.F. Hoskins, R. Robson, *J. Am. Chem. Soc.* 112 (1990) 1546.
- [40] M. Fujita, Y.J. Kwon, S. Washizu, K. Ogura, *J. Am. Chem. Soc.* 116 (1994) 1151.
- [41] O.M. Yaghi, G. Li, H. Li, *Nature* 378 (1995) 703.
- [42] D. Venkataraman, G.B. Gardner, S. Lee, J.S. Moore, *J. Am. Chem. Soc.* 117 (1995) 11600.
- [43] M. Kondo, T. Yoshitomi, K. Seki, H. Matsuzaka, S. Kitagawa, *Angew. Chem., Int. Ed. Engl.* 36 (1997) 1725.
- [44] M. Kondo, T. Okubo, A. Asami, S. Noro, T. Yoshitomi, S. Kitagawa, T. Ishii, H. Matsuzaka, K. Seki, *Angew. Chem., Int. Ed. Engl.* 38 (1999) 140.
- [45] R. Kitauro, K. Fujimoto, S. Noro, M. Kondo, S. Kitagawa, *Angew. Chem., Int. Ed. Engl.* 41 (2002) 133.
- [46] R. Kitauro, S. Kitagawa, Y. Kubota, T.C. Kobayashi, K. Kindo, Y. Mita, A. Matsuo, M. Kobayashi, H.-C. Chang, T.C. Ozawa, M. Suzuki, M. Sakata, M. Takata, *Science* 298 (2002) 23581.
- [47] R. Kitauro, R. Matsuda, Y. Kubota, S. Kitagawa, M. Takata, T.C. Kobayashi, M. Suzuki, *J. Phys. Chem. B* 109 (2005) 23378.
- [48] R. Matsuda, R. Kitauro, S. Kitagawa, Y. Kubota, T.C. Kobayashi, S. Horike, M. Takata, *J. Am. Chem. Soc.* 126 (2004) 14063.
- [49] R. Matsuda, R. Kitauro, S. Kitagawa, Y. Kubota, R.V. Belosludov, T.C. Kobayashi, H. Sakamoto, T. Chiba, M. Takata, Y. Kawazoe, Y. Mita, *Nature* 436 (2005) 238.
- [50] Y. Kubota, M. Takata, R. Matsuda, R. Kitauro, S. Kitagawa, T.C. Kobayashi, *Angew. Chem. Int. Ed.* 45 (2006) 4932.
- [51] Y. Kubota, M. Takata, R. Matsuda, R. Kitauro, S. Kitagawa, K. Kato, M. Sakata, T.C. Kobayashi, *Angew. Chem. Int. Ed.* 44 (2005) 920, S920/921–S920/924.
- [52] D. Li, K. Kaneko, *J. Phys. Chem. B* 104 (2000) 8940.
- [53] T. Uemura, S. Horike, S. Kitagawa, *Chem.: Asian J.* 1 (2006) 36.
- [54] T. Uemura, R. Kitauro, Y. Ohta, M. Nagaoka, S. Kitagawa, *Angew. Chem. Int. Ed.* 45 (2006) 4112.
- [55] IUPAC, *Pure Appl. Chem.* 31 (1972) 578.
- [56] F. Rouquerol, J. Rouquerol, K. Sing, *Adsorption by Powders and Porous Solids*, Academic Press, London, 1999.
- [57] K. Kaneko, R.F. Cracknell, D. Nicholson, *Langmuir* 10 (1994) 4606.
- [58] M.M. Dubinin, *Chem. Rev.* 60 (1960) 235.
- [59] M. Eddaoudi, J. Kim, N. Rosi, D. Vodak, J. Wachter, M. O’Keeffe, O.M. Yaghi, *Science* 295 (2002) 469.
- [60] S.-I. Noro, S. Kitagawa, M. Kondo, K. Seki, *Angew. Chem. Int. Ed.* 39 (2000) 2082.
- [61] K. Biradha, Y. Hongo, M. Fujita, *Angew. Chem. Int. Ed.* 39 (2000) 3843.
- [62] K. Biradha, M. Fujita, *Dalton* (2000) 3805.
- [63] L. Pan, H. Liu, X. Lei, X. Huang, D.H. Olson, N.J. Turro, J. Li, *Angew. Chem. Int. Ed.* 42 (2003) 542.
- [64] D.V. Soldatov, J.A. Ripmeester, S.I. Shergina, I.E. Sokolov, A.S. Zanina, S.A. Gromilov, Y.A. Dyadin, *J. Am. Chem. Soc.* 121 (1999) 4179.
- [65] L. Carlucci, G. Ciani, D.M. Proserpio, A. Sironi, *Angew. Chem., Int. Ed. Engl.* 34 (1995) 1895.
- [66] J.Y. Lu, A.M. Babb, *Chem. Commun.* (2002) 1340.
- [67] Y.-P. Ren, L.-S. Long, B.-W. Mao, Y.-Z. Yuan, R.-B. Huang, L.-S. Zheng, *Angew. Chem., Int. Ed. Engl.* 42 (2003) 532.
- [68] W. Mori, T.C. Kobayashi, J. Kurobe, K. Amaya, Y. Narumi, T. Kumada, K. Kindo, H.A. Katori, T. Goto, N. Miura, S. Takamizawa, H. Nakayama, K. Yamaguchi, *Mol. Cryst. Liq. Cryst.* 306 (1997) 1.
- [69] H. Kanoh, K. Kaneko, *J. Phys. Chem.* 100 (1996) 755.
- [70] D.N. Dybtsev, H. Chun, K. Kim, *Angew. Chem., Int. Ed. Engl.* 43 (2004) 5033.
- [71] D. Tanaka, S. Masaoka, S. Horike, S. Furukawa, M. Mizuno, K. Endo, S. Kitagawa, *Angew. Chem. Int. Ed.* 45 (2006) 4628.
- [72] O. Ohmori, M. Kawano, M. Fujita, *J. Am. Chem. Soc.* 126 (2004) 16292.
- [73] H.J. Choi, M.P. Suh, *J. Am. Chem. Soc.* 126 (2004) 15844.
- [74] J.L.C. Rowsell, E.C. Spencer, J. Eckert, J.A.K. Howard, O.M. Yaghi, *Science* 309 (2005) 1350.
- [75] G.J. Halder, C.J. Kepert, *J. Am. Chem. Soc.* 127 (2005) 7891.
- [76] T.K. Maji, G. Mostafa, R. Matsuda, S. Kitagawa, *J. Am. Chem. Soc.* 127 (2005) 17152.
- [77] M.R. Hartman, V.K. Peterson, Y. Liu, S.S. Kaye, J.R. Long, *Chem. Mater.* 18 (2006) 3221.
- [78] S. Takamizawa, T. Saito, T. Akatsuka, E. Nakata, *Inorg. Chem.* 44 (2005) 1421.
- [79] S. Takamizawa, E. Nakata, T. Saito, T. Akatsuka, *Inorg. Chem.* 44 (2005) 1362.
- [80] S. Takamizawa, E.-I. Nakata, *CrystEngComm* 7 (2005) 476.
- [81] S. Takamizawa, E.-I. Nakata, T. Saito, *Angew. Chem. Int. Ed.* 43 (2004) 1368.
- [82] S. Takamizawa, E.-I. Nakata, H. Yokoyama, K. Mochizuki, W. Mori, *Angew. Chem., Int. Ed. Engl.* 42 (2003) 4331.
- [83] H.J. Jodl, F. Bolduan, H.D. Hochheimer, *Phys. Rev. B* 31 (1985) 7376.
- [84] K. Barthelet, J. Marrot, D. Riou, G. Férey, *Angew. Chem., Int. Ed. Engl.* 41 (2002) 281.
- [85] R. Kitauro, K. Seki, G. Akiyama, S. Kitagawa, *Angew. Chem. Int. Ed.* 42 (2003) 428.
- [86] M. Rigby, *The Forces Between Molecules*, Clarendon Press, Oxford, UK, 1986.
- [87] R. Radhakrishnan, K.E. Gubbins, M. Sliwinski-Bartkowiak, *J. Chem. Phys.* 112 (2000) 11048.
- [88] S. Budavari, *The Merck Index*, 12th ed., Merck Research Laboratories, New Jersey, 1996.
- [89] H. Li, M. Eddaoudi, M. O’Keeffe, O.M. Yaghi, *Nature* 402 (1999) 276.
- [90] H.K. Chae, D.Y. Siberio-Perez, J. Kim, Y. Go, M. Eddaoudi, A.J. Matzger, M. O’Keeffe, O.M. Yaghi, *Nature* 427 (2004) 523.
- [91] X. Zhao, B. Xiao, A.J. Fletcher, K.M. Thomas, D. Bradshaw, M.J. Rosseinsky, *Science* 306 (2004) 1012.
- [92] G. Férey, M. Latroche, C. Serre, F. Millange, T. Loiseau, A. Percheron-Guegan, *Chem. Commun.* (2003) 2976.
- [93] K. Seki, W. Mori, *J. Phys. Chem. B* 106 (2002) 1380.
- [94] M. Kondo, M. Shimamura, S. Noro, S. Minakoshi, A. Asami, K. Seki, S. Kitagawa, *Chem. Mater.* 12 (2000) 1288.
- [95] K. Seki, S. Takamizawa, W. Mori, *Chem. Lett.* (2001) 332.
- [96] K. Seki, S. Takamizawa, W. Mori, *Chem. Lett.* (2001) 122.
- [97] K. Seki, *Phys. Chem. Chem. Phys.* 4 (2002) 1968.
- [98] K. Seki, *Chem. Commun.* (2001) 1496.
- [99] S.S.-Y. Chui, S.M.-F. Lo, J.P.H. Charmant, A.G. Orpen, I.D. Williams, *Science* 283 (1999) 1148.
- [100] L.C. Tabares, J.A.R. Navarro, J.M. Salas, *J. Am. Chem. Soc.* 123 (2001) 383.
- [101] D.V. Soldatov, J.A. Ripmeester, *Chem. Mater.* 12 (2000) 1827.
- [102] J.S. Seo, D. Whang, H. Lee, S.I. Jun, J. Oh, Y.J. Jeon, K. Kim, *Nature* 404 (2000) 982.
- [103] M. Eddaoudi, H. Li, O.M. Yaghi, *J. Am. Chem. Soc.* 122 (2000) 1391.
- [104] W. Mori, H. Hoshino, Y. Nishimoto, S. Takamizawa, *Chem. Lett.* (1999) 331.
- [105] P.M. Forster, J. Eckert, J.-S. Chang, S.-E. Park, G. Férey, A.K. Cheetham, *J. Am. Chem. Soc.* 125 (2003) 1309.
- [106] M. Fujita, J.Y. Kwon, S. Washizu, K. Ogura, *J. Am. Chem. Soc.* 116 (1994) 1151.
- [107] R. Tannenbaum, *Chem. Mater.* 6 (1994) 550.
- [108] B. Gomez-Lor, E. Gutiérrez-Puebla, M. Iglesias, M.A. Monge, C. Ruiz-Valero, N. Snejko, *Inorg. Chem.* 41 (2002) 2429.
- [109] J.M. Tanski, P.T. Wolczanski, *Inorg. Chem.* 40 (2001) 2026.
- [110] O.R. Evans, H.L. Ngo, W. Lin, *J. Am. Chem. Soc.* 123 (2001) 10395.
- [111] M. Dinca, J.R. Long, *J. Am. Chem. Soc.* 127 (2005) 9376.
- [112] S.S. Kaye, J.R. Long, *J. Am. Chem. Soc.* 127 (2005) 6506.
- [113] K. Uemura, K. Saito, S. Kitagawa, H. Kita, *J. Am. Chem. Soc.* 128 (2006) 16122.
- [114] K. Yamada, H. Tanaka, S. Yagishita, K. Adachi, T. Uemura, S. Kitagawa, S. Kawata, *Inorg. Chem.* 45 (2006) 4322.
- [115] S. Shimomura, R. Matsuda, T. Tsujino, T. Kawamura, S. Kitagawa, *J. Am. Chem. Soc.* 128 (2006) 16416.
- [116] M. Dinca, A. Dailly, Y. Liu, C.M. Brown, D.A. Neumann, J.R. Long, *J. Am. Chem. Soc.* 128 (2006) 16876.

- [117] M. Dinca, A.F. Yu, J.R. Long, *J. Am. Chem. Soc.* 128 (2006) 8904.
- [118] S. Kitagawa, K. Uemura, *Chem. Soc. Rev.* 34 (2005) 109.
- [119] K. Uemura, R. Matsuda, S. Kitagawa, *J. Solid State Chem.* 178 (2005) 2420.
- [120] M.J. Rosseinsky, *Micropor. Mesopor. Mater.* 73 (2004) 15.
- [121] M.P. Suh, Y.E. Cheon, *Aust. J. Chem.* 59 (2006) 605.
- [122] A.J. Fletcher, K.M. Thomas, M.J. Rosseinsky, *J. Solid State Chem.* 178 (2005) 2491.
- [123] K. Biradha, M. Fujita, *Angew. Chem., Int. Ed. Engl.* 41 (2002) 3392.
- [124] L.G. Beauvais, M.P. Shores, J.R. Long, *J. Am. Chem. Soc.* 122 (2000) 2763.
- [125] K. Biradha, Y. Hongo, M. Fujita, *Angew. Chem., Int. Ed. Engl.* 41 (2002) 3395.
- [126] M.P. Suh, J.W. Ko, H.J. Choi, *J. Am. Chem. Soc.* 124 (2002) 10976.
- [127] C.J. Kepert, D. Hesek, P.D. Beer, M.J. Rosseinsky, *Angew. Chem. Int. Ed.* 37 (1998) 3158.
- [128] B.F. Abrahams, P.A. Jackson, R. Robson, *Angew. Chem., Int. Ed. Engl.* 37 (1998) 2656.
- [129] A.J. Fletcher, E.J. Cussen, T.J. Prior, M.J. Rosseinsky, C.J. Kepert, K.M. Thomas, *J. Am. Chem. Soc.* 123 (2001) 10001.
- [130] C.J. Kepert, M.J. Rosseinsky, *Chem. Commun.* (1999) 375.
- [131] S.K. Makinen, N.J. Melcer, M. Parvez, G.K.H. Shimizu, *Chem. Eur. J.* 7 (2001) 5176.
- [132] J.-H. Liao, S.-H. Cheng, C.-T. Su, *Inorg. Chem. Commun.* 5 (2002) 761.
- [133] C. Serre, F. Millange, C. Thouvenot, M. Nogues, G. Marsolier, D. Louer, G. Férey, *J. Am. Chem. Soc.* 124 (2002) 13519.
- [134] T.K. Maji, K. Uemura, H.-C. Chang, R. Matsuda, S. Kitagawa, *Angew. Chem., Int. Ed. Engl.* 43 (2004) 3269.
- [135] E.J. Cussen, J.B. Claridge, M.J. Rosseinsky, C.J. Kepert, *J. Am. Chem. Soc.* 124 (2002) 9574.
- [136] E.Y. Lee, S.Y. Jang, M.P. Suh, *J. Am. Chem. Soc.* 127 (2005) 6374.
- [137] H. Kim, M.P. Suh, *Inorg. Chem.* 44 (2005) 810.
- [138] S.-I. Noro, S. Horike, D. Tanaka, S. Kitagawa, T. Akutagawa, T. Nakamura, *Inorg. Chem.* 45 (2006) 9290.
- [139] S. Horike, R. Matsuda, D. Tanaka, S. Matsubara, M. Mizuno, K. Endo, S. Kitagawa, *Angew. Chem. Int. Ed.* 45 (2006) 7226.
- [140] S.-I. Noro, R. Kitaura, M. Kondo, S. Kitagawa, T. Ishii, H. Matsuzaka, M. Yamashita, *J. Am. Chem. Soc.* 124 (2002) 2568.
- [141] S.-I. Noro, S. Kitagawa, *Stud. Surf. Sci. Catal.* 141 (2002) 363.
- [142] D.V. Soldatov, A.T. Henegouwen, G.D. Enright, C.I. Ratcliffe, J.A. Ripmeester, *Inorg. Chem.* 40 (2001) 1626.
- [143] A.Y. Manakov, D.V. Soldatov, J.A. Ripmeester, J. Lipkowski, *J. Phys. Chem. B* 104 (2000) 12111.
- [144] K. Uemura, S. Kitagawa, M. Kondo, K. Fukui, R. Kitaura, H.-C. Chang, T. Mizutani, *Chem.: Eur. J.* 8 (2002) 3586.
- [145] K. Uemura, S. Kitagawa, K. Fukui, K. Saito, *J. Am. Chem. Soc.* 126 (2004) 3817.
- [146] F. Millange, C. Serre, G. Férey, *Chemical Communications*, Cambridge, United Kingdom, 2002, p. 822.
- [147] P.L. Llewellyn, S. Bourrrelly, C. Serre, Y. Filinchuk, G. Férey, *Angew. Chem. Int. Ed.* 45 (2006) 7751.
- [148] C. Mellot-Draznieks, C. Serre, S. Surble, N. Audebrand, G. Férey, *J. Am. Chem. Soc.* 127 (2005) 16273.
- [149] D. Li, K. Kaneko, *Chem. Phys. Lett.* 335 (2001) 50.
- [150] A. Kondo, H. Noguchi, S. Ohnishi, H. Kajiro, A. Tohdoh, Y. Hattori, W.-C. Xu, H. Tanaka, H. Kanoh, K. Kaneko, *Nano Letters* 6 (2006) 2581.
- [151] E. Lee, J. Kim, J. Heo, D. Whang, K. Kim, *Angew. Chem., Int. Ed. Engl.* 40 (2001) 399.
- [152] A. Kamiyama, T. Noguchi, T. Kajiwar, T. Ito, *Angew. Chem., Int. Ed. Engl.* 39 (2000) 3130.
- [153] O.M. Yaghi, H. Li, T.L. Groy, *Inorg. Chem.* 36 (1997) 4292.
- [154] B.H. Hamilton, K.A. Kelly, T.A. Wagler, M.P. Espe, C.J. Ziegler, *Inorg. Chem.* 41 (2002) 4984.
- [155] O.-S. Jung, Y.J. Kim, K.M. Kim, Y.-A. Lee, *J. Am. Chem. Soc.* 124 (2002) 7906.
- [156] K.S. Min, M.P. Suh, *J. Am. Chem. Soc.* 122 (2000) 6834.
- [157] O.-S. Jung, Y.J. Kim, Y.-A. Lee, H.K. Chae, H.G. Jang, J. Hong, *Inorg. Chem.* 40 (2001) 2105.
- [158] O.-S. Jung, Y.J. Kim, Y.-A. Lee, K.H. Yoo, *Chem. Lett.* (2002) 500.
- [159] L. Pan, E.B. Woodlock, X. Wang, K.-C. Lam, A.L. Rheingold, *Chem. Commun.* (2001) 1762.
- [160] A.N. Khlobystov, N.R. Champness, C.J. Roberts, S.J.B. Tendler, C. Thompson, M. Schröer, *CrystEngComm* 4 (2002) 426.
- [161] O.-S. Jung, Y.J. Kim, Y.-A. Lee, J.K. Park, H.K. Chae, *J. Am. Chem. Soc.* 122 (2000) 9921.
- [162] O.-S. Jung, Y.J. Kim, Y.-A. Lee, K.-M. Park, S.S. Lee, *Inorg. Chem.* 42 (2003) 844.
- [163] X. Xu, M. Nieuwenhuyzen, S.L. James, *Angew. Chem., Int. Ed. Engl.* 41 (2002) 764.
- [164] T.K. Maji, R. Matsuda, S. Kitagawa, *Nat. Mater.* 6 (2007) 142.
- [165] J. Gonzalez, R. Nandini Devi, D.P. Tunstall, P.A. Cox, P.A. Wright, *Micropor. Mesopor. Mater.* 84 (2005) 97.
- [166] S. Takamizawa, E.-I. Nakata, T. Akatsuka, *Angew. Chem. Int. Ed.* 45 (2006) 2216.
- [167] S. Kitagawa, *Nature* 441 (2006) 584.
- [168] H. Chun, D.N. Dybtsev, H. Kim, K. Kim, *Chem.: Eur. J.* 11 (2005) 3521.
- [169] T. Uemura, Y. Hoshino, S. Kitagawa, K. Yoshida, S. Isoda, *Chem. Mater.* 18 (2006) 992.
- [170] T. Uemura, S. Kitagawa, *J. Am. Chem. Soc.* 125 (2003) 7814.
- [171] T. Uemura, M. Ohba, S. Kitagawa, *Inorg. Chem.* 43 (2004) 7339.
- [172] S. Masaoka, D. Tanaka, H. Kitahata, S. Araki, R. Matsuda, K. Yoshikawa, K. Kato, M. Takata, S. Kitagawa, *J. Am. Chem. Soc.* 128 (2006) 15799.
- [173] C.-D. Wu, A. Hu, L. Zhang, W. Lin, *J. Am. Chem. Soc.* 127 (2005) 8940.
- [174] M.P. Suh, H.R. Moon, E.Y. Lee, S.Y. Jang, *J. Am. Chem. Soc.* 128 (2006) 4710.
- [175] H.R. Moon, J.H. Kim, M.P. Suh, *Angew. Chem. Int. Ed.* 45 (2005) 1261.